THE AMPACITY AND THERMAL PERFORMANCE OF DISTRIBUTION CABLE IN UNDERGROUND SYSTEMS

A Thesis

Presented To

The Faculty of Graduate Studies

University of Manitoba

In Partial Fulfillment

of the Requirements for the Degree

Master of Science

Electrical Engineering Department

by

Darryl F. Bukoski

June 1981

THE AMPACITY AND THERMAL PERFORMANCE OF DISTRIBUTION CABLE IN UNDERGROUND SYSTEMS

BY

DARRYL F. BUKOSKI

A thesis submitted to the Faculty of Graduate Studies of the University of Manitoba in partial fulfillment of the requirements of the degree of

MASTER OF SCIENCE

ABSTRACT

Theoretical equations for calculating the electrical characteristics and thermal properties of power cables in underground duct bank systems are developed. Analytical techniques are applied to represent the cable system by a series of linear equations under steady state conditions. A computer program is developed to calculate the cable system parameters and generate a coefficient matrix in terms of the linear equations. This matrix is solved and the ampacity or conductor temperature for each cable is calculated. The effects of various cable system parameters on cable ampacity are discussed. Conclusions and recommendations on the results and on the method of analysis are made.

ACKNOWLEDGEMENTS

The author wishes to take this opportunity to express his appreciation for the guidance and assistance of Dr. R. W. Menzies who acted as adviser for the thesis.

The author extends a thank you to Winnipeg Hydro for providing the facilities and to the personnel who conducted the tests.

Thanks are also extended to Mr. Hugh MacDiarmid and to Mr. Jack McMath for their comments and for providing useful literature.

The author would also like to thank Mr. Harry Pagut for drafting the illustrations, and Mrs. Lori Spack for her excellent job of typing the thesis.

To my wife Lorraine for her patience, understanding and words of encouragement during the long period of preparation for the thesis, a special "Thank You".

TABLE OF CONTENTS

PAGE

APPENDICES

LIST OF FIGURES

LIST OF TABLES

LIST OF SYMBOLS

A	area, CM
A,B,C	duct constants
A,B	matrices
a,b	temperature correction factors
α_e	earth thermal diffusivity, in ^{2}/hour
Cos Ø	power factor of cable dielectirc
C	capacitance of cable dielectric, μF/ft
D	diameter, in
D_c	outside of conductor
D_i	outside of insulation
D_j	outside of jacket
D_o	inside of annular conductor
D_{sm}	mean diameter of sheath
D_w	inside of duct wall
D_x	fictitious diameter at which the effect of loss factor commences
d,d'	distance, in
E	applied voltage across dielectric, kV
ϵ	coefficient of surface emissivity
ϵ_r	relative perittivity of the insulation
f	frequency, hertz
F(Xs)	skin effect function, p.u.
F(Xp)	Bessel function for proximity effect, p.u.
F_{ld}	load factor, p.u.
F_{ls}	loss factor, p.u.
G	geometric factor, p.u.
G_i	insulation
G_j	jacket

G_w	duct wall
$\mathbf{I}$	conductor current matrix
I	conductor current, A
I_c	capacitive current
I_E	leakage current
I_T	$= I_E + I_C$
J	current density, A/CM
$\mathbf{K}$	coefficient matrix
K_p	relative transverse conductivity factor, p.u.
K_s	skin effect correction factor, p.u.
l	length, ft
L_b	depth of burial to centre of duct bank, in
P	pressure , psi
p	point location
q,Q	rate of heat flow, W
q	ratio of the sum of the losses in the conductor and sheath to the losses in the conductor, p.u.
r,r_1,r_2	radii, in
R_{ac}, R'	conductor ac resistance , Ω/ft
R_{dc}, R'_{dc}	conductor dc resistance , Ω/ft
R_s	sheath ac resistance , Ω/ft
$\bar{R}$, $\bar{R}', \bar{R}'', \bar{R}'''$	thermal resistance , ^{o}C ft/W
$\bar{R}_b$	duct bank (concrete)
$\bar{R}_{dx}$	duct bank to diameter D_x
$\bar{R}_e$	ambient earth
$\bar{R}_i$	insulation
$\bar{R}_j$	jacket
$\bar{R}_{sd}$	between cable surface and surrounding duct

$\bar{R}_w$	duct wall
$\bar{R}_{12}, \bar{R}_{13}$, etc.	between interference ducts
r_b	equivalent radius of duct bank, in
ρ	electrical resistivity, CM Ω/ft
ρ_c, ρ_2, ρ_2'	conductor
ρ_s	sheath
$\bar{\rho}$	thermal resistivity, ^{o}C cm/W
$\bar{\rho}_b$	duct bank (concrete)
$\bar{\rho}_e$	ambient earth
$\bar{\rho}_i$	insulation
$\bar{\rho}_j$	jacket
$\bar{\rho}_w$	duct wall
S	spacing between adjacent conductors, in
T	temperature of zero resistance, ^{o}C
T_a	earth ambient temperature, ^{o}C
ΔT	conductor temperature rise, ^{o}C
ΔT_c	due to conductor loss
ΔT_d	due to dielectric loss
ΔT_s	due to sheath loss
T_m	mean temperature of duct air space, ^{o}C
t	thickness, in
t_i	insulation
t_j	jacket
t_w	duct wall
t_1, t_2	temperatures, ^{o}C
V	cable line-to-line operating voltage, kV
W	heat loss, W/ft
W_c	conductor I^2R loss

W_d	dielectric
W_{sc}	sheath circulating current
W_{se}	sheath eddy currents
W_s	$= W_{sc} + W_{se}$
ω	$= 2\pi f$
X	smaller duct bank dimension, in
X	matrix
X_m	mutual reactance
ΔX	distance, in
y	larger duct bank dimension, in
Y_c	$= 1.0 + Y_{cp} + Y_{cs}$, p.u.
Y_{cp}	proximity effect factor, p.u.
Y_{cs}	skin effect factor, p.u.
Y_s	$= Y_{sc} + Y_{se}$, p.u.
Y_{sc}	sheath circulating current factor, p.u.
Y_{ce}	sheath eddy current factor, p.u.
A	ampere
^oC	degrees Centigrade
CM	circular mil
ft	foot
in	inch
kV	kilovolt
μF	microfarad
Ω	ohm
p.u.	per unit
psi	pounds per square inch
W	watt

CHAPTER 1

INTRODUCTION

The major restriction on the current rating, or ampacity, of a power cable is the temperature rise which the cable insulation may achieve without being permanently damaged. The insulation is adjacent to the conductor and its temperature limit determines the conductor maximum operating temperature.

The conductor temperature rise is dependent on the cable heat loss, the characteristics of the thermal environment and the effects of heat from other cables. The first practical calculation of the temperature rise for buried cables was presented by A. E. Kennelly in 1893. He expressed the conductor temperature rise as a function of the cable heat loss, cable geometry and the thermal resistivity of the earth.

Numerous techniques for evaluating cable performance in underground systems have been developed in the intervening years. The National Edison Light Association (NELA) developed a table of duct heat constants in 1930 to account for cable heating in duct banks. D. M. Simmons published a paper in 1932 for evaluating cable ampacities based on the NELA duct constants and the mathematical data and equations relating to the electrical problems of underground cables scattered throughout the literature at that time. The method was adequate but it did not provide a technique for detailed analysis.

Throughout the 1940's and 50's various papers were

published outlining analytical techniques for calculating various cable system parameters. In 1957 J. H. Neher and M. H. McGrath published a paper detailing procedures for calculating the ampacities for identical cables with similar operating characteristics in an underground system. This method became the basis for evaluating cable loading capacity.

In 1962 the Insulated Power Cable Engineers Association (IPCEA) in conjunction with the American Institute of Electrical Engineers (AIEE) published tables of ampacities for a wide range of cable constructions, voltages, and installations based on methods summarized by Neher and McGrath. These tables were updated in 1967 to reflect the higher operating temperatures established by the Association of Edison Illuminating Companies (AEIC) for impregnated paper insulated cables. Tables similar to these are used presently to provide general guide lines for rating cables with identical characteristics but they don't offer the flexibility to analyze the thermal performance of actual installations.

This thesis is written with the objective of developing an analytical technique that may be used to analyze actual installations under any steady state operating condition. The physical construction of the duct bank, the types of cables installed, the operating characteristics of each cable, the effects of each cable on other cables and the thermal properties are some of the more important

cable system parameters that are included in the analysis. The cable system is described by a series of linear equations, which account for the various cable system parameters. These equations are solved and the thermal performance or ampacity for each cable in the duct bank is calculated.

Similar analytical methods to those outlined by Neher and McGrath are developed in chapters one and two to calculate the electrical characteristics and thermal properties for the cable system. The procedures outlined in chapter three develop a system of linear equations in terms of the unknown quantity, either conductor temperature or current, for each cable. Chapter four describes a computer program in terms of high level flow charts which solves these equations. Chapter five discusses the effects of various cable parameters on cable ampacities for a typical cable system. Some results are compared with cable rating tables and field measurements. Conclusions and recommendations are stated in chapter six.

CHAPTER 2

ELECTRICAL CHARACTERISTICS OF CABLE

2.0 Introduction

This chapter develops equations for calculating the amount of heat loss generated in a power cable. This heat loss is a function of the operating voltage, and the current being conducted by the conductor and sheath. The conductor resistance, sheath resistance and cable dielectric interact with the voltage and currents to generate losses. These losses produce a temperature rise in the cable and ultimately are used to evaluate the cable current carrying capacity.

Numerous types of cable construction are utilized for transmission and distribution of electric power. Each type, of course, has its own particular characteristics which require individual evaluation. For simplicity the discussion in this chapter and throughout the thesis applies only to single conductor paper insulated cable, as shown in figure 2.1, which is used in three phase circuits. Information for other types of cable construction may be found in many of the references listed at the end of this thesis.

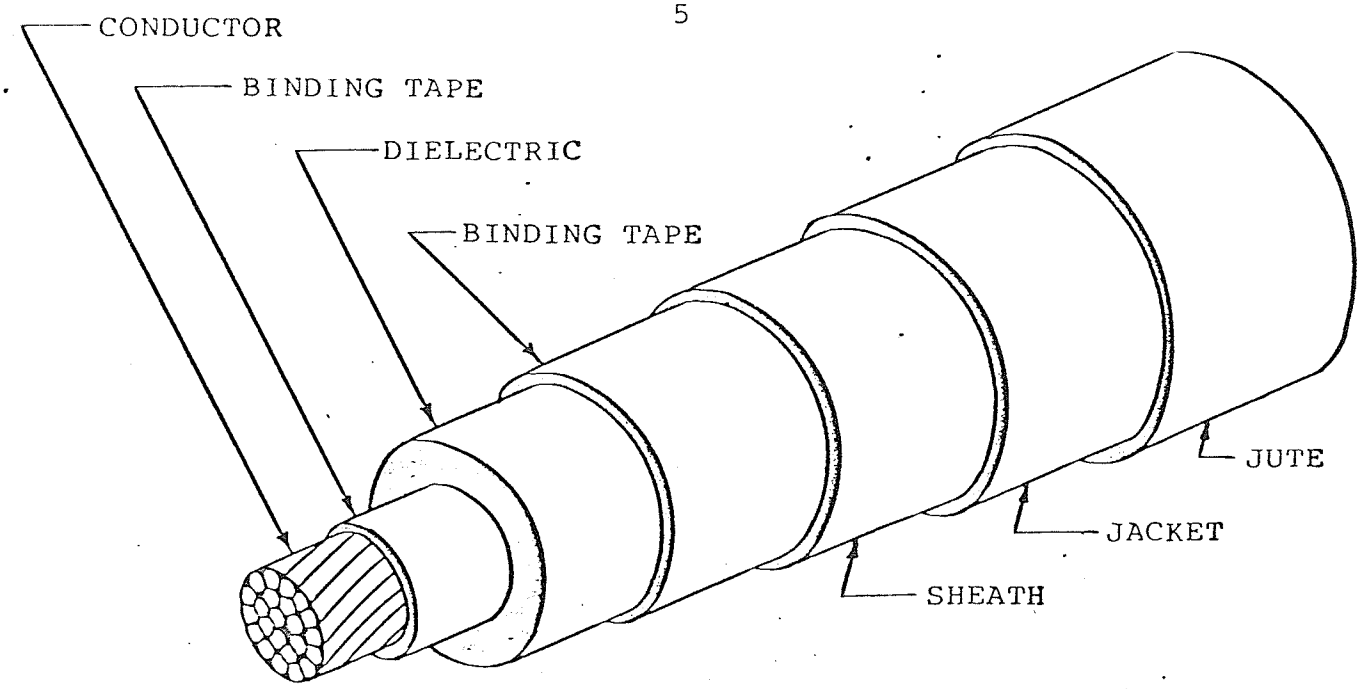

FIGURE 2.1 - TYPICAL SINGLE CONDUCTOR CABLE

2.1 DC Resistance of the Conductor

The dc Resistance R_{dc} of a conductor is defined as

$$R_{dc} = \frac{\text{power loss in conductor}}{[\text{dc current}]^2} \qquad (2.1)$$

The dc resistance can also be calculated by

$$R_{dc} = \frac{\rho_c}{A} \quad \Omega/\text{ft} \qquad (2.2)$$

where ρ_c is the electrical resistivity of the conductor.

Most large conductors in power cables are stranded or segmented to facilitate easier cable bending and to reduce the ac skin effect. R_{dc} is increased because spiralling of these wires causes the effective conductor length to increase. This phenomenon is difficult to determine analytically because of the unknown path of the conductor current. Some current flows from strand to strand while some follows the spiralling

of the conductor. The fraction of the total current which does flow from strand to strand is dependent on the cleanliness of the conductor, tension, oxidation, movement and conductor construction. It is customary to increase R_{dc} by a lay factor of 2% to account for this stranding effect.

Variations in conductor temperature cause the resistance to change according to the following equation:

$$\frac{R_{dc}'}{R_{dc}} = \frac{\rho_2'}{\rho_2} = \frac{T + t_2}{T + t_1} \qquad (2.3)$$

Some examples of conductor electrical resistivities and absolute temperatures for zero resistance are shown in Table 2.1.

Generally, the dc resistance of a particular cable is specified by the cable manufacture. However, it may also be obtained with sufficient accuracy from general information tables for various conductor sizes (1).

Material	ρ, CM Ω/ft at 25°C	T, °C
Copper, 100% Conductivity	10.57	234.5
Aluminum, 100% Conductivity	17.36	228.1
Lead, 7.84% Conductivity	134.88	236.

TABLE 2.1 - ELECTRICAL RESISTIVITIES OF VARIOUS MATERIALS

2.2 AC Resistance of the Conductor

A conductor offers a greater resistance to the flow of ac current than it does to dc current. The magnitude of the increase usually is expressed as an "ac/dc ratio". The resistance is increased because of the following inductive components:

i. skin effect - the tendency of alternating current to crowd toward the surface of the conductor, and

ii. proximity effect - the distortion of current distribution in the conductor due to the magnetic effects of other nearby currents.

Pipe type cables or conductors installed in metallic conduit will also experience increased ac resistance. However, these types of installations are not considered in this manuscript.

2.2.1 Skin Effect

Unequal current distribution in a single isolated conductor is caused by the continuously varying magnetic field of the ac current flowing in the conductor itself. The inductance increases towards the centre of the conductor and the effect causes the current density J to decrease towards the centre accordingly, as shown in figure 2.2. The result is an overall increase in resistance for conductors with time-varying currents. This is known as the skin effect. (2)

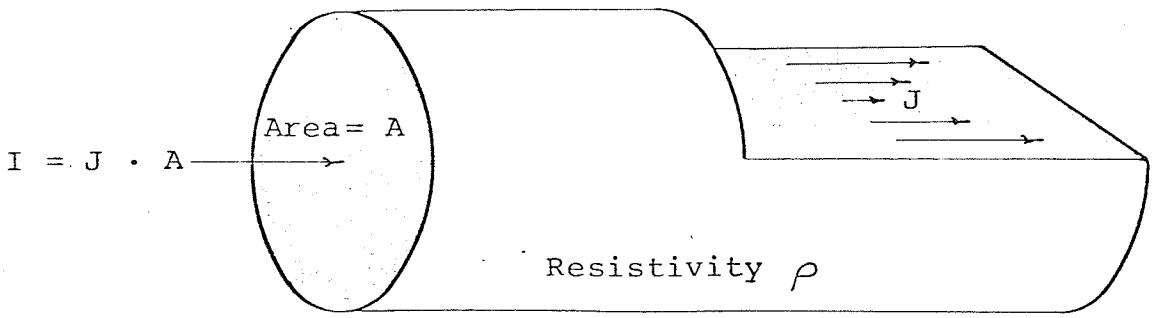

Figure 2.2 -CONDUCTOR SKIN EFFECT

The problem of calculating the increase in resistance has been extensively treated in numerous technical articles and the skin effect of many shapes of conductors may be found from curves and formulas therein. However for simplicity the skin effect factor has been approximated by IPCEA (3) by the following equation:

$$Y_{cs} = F(X_s) = \frac{11.0}{\left[\frac{R_{dc}}{K_s} + \frac{4K_s}{R_{dc}} - 2.56\left[\frac{K_s}{R_{dc}}\right]^2\right]^2} \text{ p.u.} \qquad (2.4)$$

The factor K_s accounts for the shape of the conductor. Typical values of K_s are shown in Table 2.2. Y_{cs} represents the per unit incremental increase of conductor ac resistance due to the skin effect.

Conductor Construction	K_s p.u.	K_p p.u.
Concentric Round	1.0	1.0
Compact Round	1.0	0.6
Compact Segmental	0.435	0.6
Compact Sector	1.0	0.3
Annular	See note	1.0

NOTE: $K_s = \frac{D_c - D_o}{D_c + D_o}\left[\frac{D_c + 2D_o}{D_c + D_o}\right]^2$

TABLE 2.2 - RECOMMENDED VALUES OF K_s and K_p

2.2.2 Proximity Effect

The flux linking a conductor current to a nearby current distorts the cross sectional current distribution in the conductor in a similar manner to skin effect, as shown in figure 2.3. The flux density J is greatest between facing surfaces where the conductor current density increases with increasing flux density. The result is an unequal flux linkage between conductor surfaces and this results in a non-uniform reactance throughout the conductor. This effectively increases the conductor ac resistance and is called the proximity effect (4).

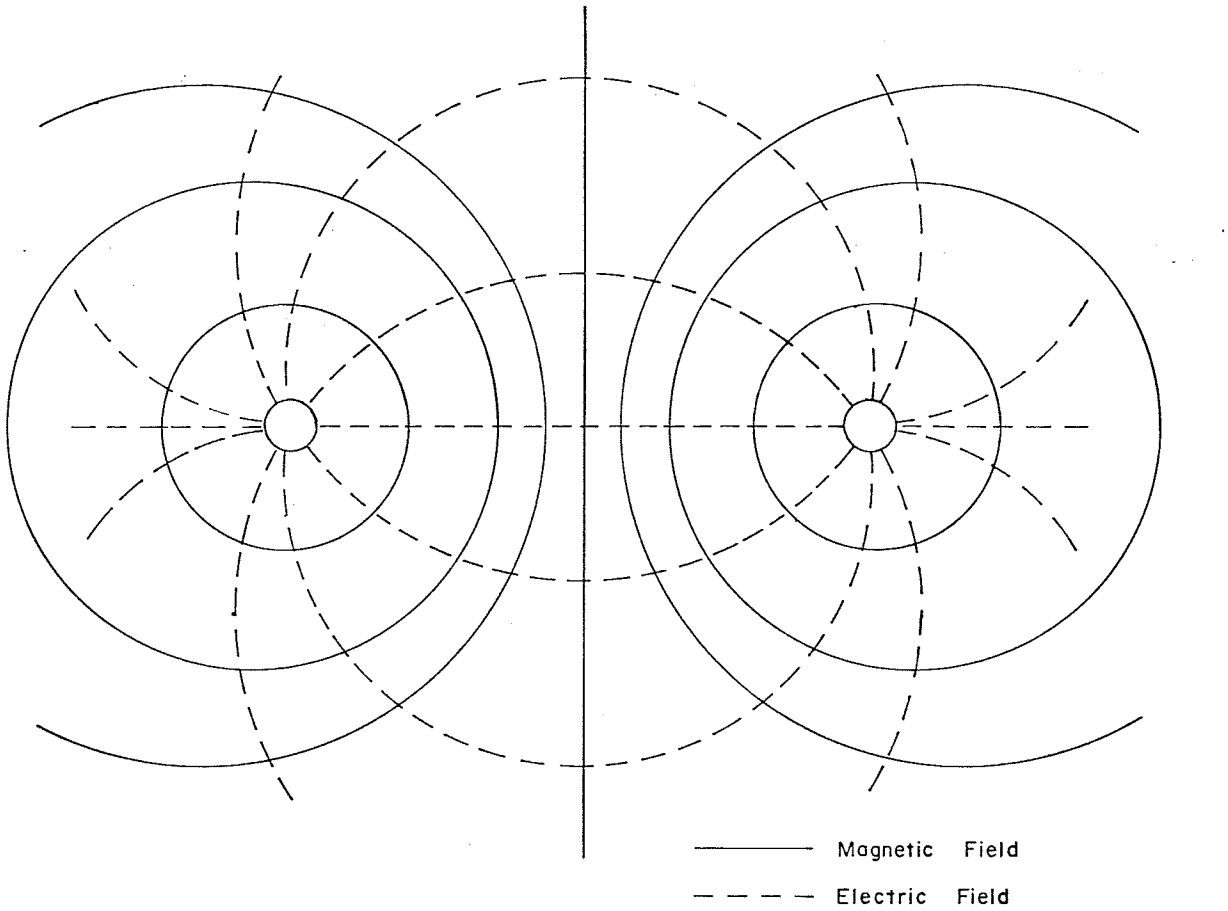

FIGURE 2.3 - CONDUCTOR PROXIMITY EFFECT

The proximity effect for a three phase circuit comprised of single conductor cables in equilateral formation in the same or separate conduits is approximated by an expression given by Arnold (5) as

$$Y_{cp} = F(X_p) \left[\frac{D_c}{S}\right]^2 \left[\frac{1.18}{F(X_p) + 0.27} + 0.312 \left[\frac{D_c}{S}\right]^2\right] \quad (2.5)$$

The derived Bessel function $F(X_p)$ is calculated by a similar equation which is used for the skin effect factor, namely,

$$F(X_p) = \frac{11.0}{\left[\frac{R_{dc}}{K_p} + \frac{4K_p}{R_{dc}} - 2.56 \left[\frac{K_p}{R_{dc}}\right]^2\right]^2} \text{ p.u.} \quad (2.6)$$

Typical values of K_p are given in Table 2.2

Y_{cs} represents the per unit incremental increase of conductor ac resistance due to the skin effect and, similarily, Y_{cp} is the per unit incremental increase of ac resistance caused by the proximity effect. Therefore, the ac resistance of the conductor becomes;

$$R_{ac} = Y_c \; R_{dc} \quad \Omega/\text{ft} \quad (2.7)$$

where,

$$Y_c = 1.0 + Y_{cs} + Y_{cp} \text{ p.u.} \quad (2.8)$$

2.3 Heat Loss In the Conductor

The heat W_c generated in the conductor is given by

$$W_c = I^2 R_{ac} \quad \text{W/ft} \quad (2.9)$$

Express in terms of the conductor dc resistance and the actual conductor temperature t_2

$$W_c = I^2 R_{dc} (1 + Ycs + Ycp) \frac{T + t_2}{T + t_1} \text{ W/ft} \quad (2.10)$$

where R_{dc} is specified at temperature t_1, usually 25° C.

2.4 Electrical Insulation of the Cable

Many materials are used as electrical insulation, or dielectric, for power cables. Natural and synthetic rubber compounds, varnished cambric, impregnated paper, polyvinyl chloride and polyethylene are some of the more common insulations.

Impregnated paper is the most common form of insulation for cables used for bulk power transmission and distribution. It consists of multiple layers of paper tapes wrapped helically around the conductor. Impregnated paper insulation has good electrical properties and excellent electrical stability over a wide range of operating temperatures. Since the insulation is in near proximity to the conductor, usually separated only by binding tape, its safe maximum operating temperature determines the cable operating temperature limits. Exceeding these limits will result in insulation deterioration, reduced dielectric strength and subsequent cable failure.

The power factor of the cable insulation, or dielectric, is defined as:

$$\frac{\text{losses in dielectric (watts)}}{\text{apparent power (volt-amperes)}}$$

When voltage is applied across a perfect dielectric there is no dielectric loss, but there is an induced capacitive current I_C which is 90^o out of phase and leading the voltage. In practice, however, a small leakage current I_E exists. This current is in phase with the applied voltage E so that the vector sum I_T of these two currents leads the voltage by less than 90^o as shown in figure 2.4. The cosine of the angle Ø, called the power factor of the dielectric, provides a sensitive measure of the quality of the cable dielectric. Typically, the power factor of impregnated paper insulated cable is 0.003pu.

POWER FACTOR

$= \cos\text{Ø}$

$= \frac{I_E}{I_T}$

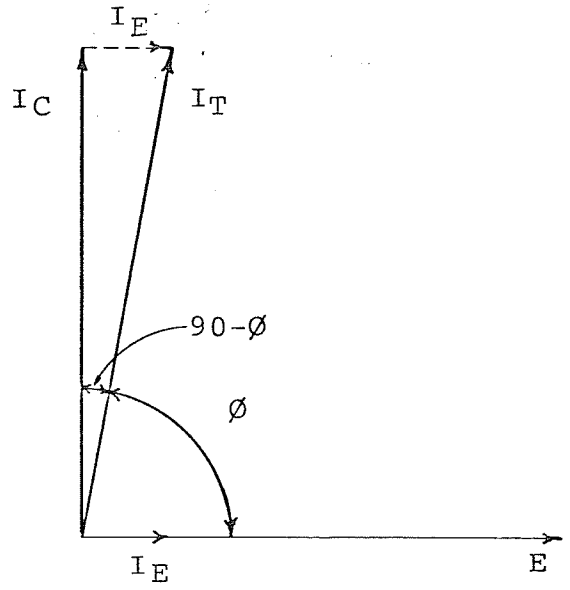

FIGURE 2.4 - DIELECTRIC POWER FACTOR

The power factor of the insulation usually increases as the cable ages, and it becomes increasingly more critical, especially at higher operating voltages. Usually conservative values of power factor which include the effects of cable ageing are applied when calculating the heat generated in the dielectric.

The manner of installation, the exposure of the insulation to air and moisture, the operating temperature of the cable conductor and the materials used in the accessories (cable joints, potheads) also affect the insulation power factor. In certain situations, the power factor increases very steeply with temperature and may result in the possibility of insulation failure due to cumulative heating.

The dielectric power factor should be based on the maximum allowable conductor temperature as shown in Table 2.3 (3) for cables rated 138 kV or less.

Cables above 138 kV require special consideration because of the increased effect of power factor on cable losses, but they are not considered here.

Dielectric Type	Power Factor p.u.				ϵ_r
	60 °C	80 °C	100 °C	115 °C	
Paper, solid type belted	0.02	0.04	0.07	0.10	3.7
Paper, solid type shielded	0.015	0.03	0.05	0.07	3.7
Paper, low pressure oil filled	0.004	0.006	0.009	0.013	3.7

TABLE 2.3 - DIELECTRIC POWER FACTOR AND SPECIFIC INDUCTIVE CAPACITY

2.5 Heat Loss in the Cable Insulation

Dielectric, or insulation, heat loss in a power cable is caused by the resistance of the dielectric to the flow of charging current. This heat is produced in the cable as a function of voltage and is independent of conductor load current. This heat loss causes an effective temperature rise of the dielectric, reduces the temperature rise available for conductor losses, and thus reduces the overall cable load current carrying capacity.

The effect of dielectric loss is included in cable loading calculations by assuming the following:

i. that the power factor throughout the entire dielectric is the same as that at the hottest point, and

ii. that the heat loss is concentrated at the conductor and must flow outward through the entire thermal path.

However, it has been shown by Simmons (6) that the temperature rise across the insulation is half as large for a given dielectric loss as for the same loss in the conductor.

The dielectric loss for a single conductor cable is

$$W_d = CV^2 \cos \phi \quad W/ft \tag{2.11}$$

where

$$C = \frac{1.687 \ \epsilon_r}{\ln \left[\frac{D_c + 2ti}{D_c}\right]} \times 10^{-5} \ \mu F/ft \tag{2.12}$$

combining both equations,

$$W_d = \frac{0.00636 \ V^2 \ \epsilon_r \cos \phi}{\ln \left[\frac{D_c + 2ti}{D_c}\right]} \quad W/ft \qquad (2.13)$$

Typical values for the relative permittivity ϵ_r and insulation power factor cos Ø are given in Table 2.3. The dielectric loss is dependent on the type of cable insulation and the cable construction. Equations for dielectric loss for other types of cable are given in the Canada Wire Power Cable Handbook (7).

2.6 Heat Loss in the Cable Sheath

Cable heat losses in the sheath are caused by longtitudinal circulating currents and by eddy currents.

2.6.1 Sheath Circulating Current

Conductor current induces voltage in the metallic sheath, usually lead or aluminum, along the length of the cable. If both ends of the sheath of a cable are grounded or connected to sheaths of adjacent cables and grounded, current will also flow in the sheath. This current will contribute to the overall heating of the cable.

For single conductor cables in trefoil formation, with sheaths bonded at both ends, the sheath circulating current I_s is given by (proof in Appendix A1):

$$I_s = I \frac{X_m}{\sqrt{X_m^2 + R_s^2}} \quad A \qquad (2.14)$$

where

$$X_m = 0.323\,\omega \ln\left[\frac{2S}{D_{sm}}\right] \Omega/\text{ft} \qquad (2.15)$$

and

$$D_{sm} = D_s - t_s \quad \text{in} \qquad (2.16)$$

The heat produced in the sheath is given by;

$$W_{sc} = I_s^2 R_s$$

$$= I^2 \frac{X_m^2}{X_m^2 + R_s^2} R_s \quad \text{W/ft} \qquad (2.17)$$

where the sheath resistance may be calculated by

$$R_s = \frac{\rho_s}{A} \quad \Omega/\text{ft} \qquad (2.18)$$

The mutual reactance X_m can be calculated for cables in different conductor arrangements by the equations given by Simmons (8).

Large circulating currents can result with short circuited sheath operation, especially with appreciable spacing between metallic sheathed single conductor cables. These currents can almost double the cable losses. Special sheath bonding for single conductor cables to reduce the sheath currents are discussed in Chapter 3 of the "Underground Systems Reference Book" (1). Generally, sheath bonding is usually restricted to triplex cables or three single conductor cables contained in the same duct. Therefore,

for most practical cases, the sheath circulating current losses are neglected for open circuited, or cross bonded sheath operation.

2.6.2 Sheath Eddy Current

The effect of sheath eddy currents for single conductor cables in equilateral configurations with open circuited lead sheaths is approximated by Neher et al (9) as;

$$W_{se} = I^2 \frac{3}{R_s} \left[\frac{D_{sm}}{2S}\right]^2 \left[\frac{f}{5.2}\right]^2 \left[1 + \frac{5}{12}\left[\frac{D_{sm}}{2S}\right]^2\right] \quad \text{W/ft} \qquad (2.19)$$

where

$$D_{sm} = D_s - t_s \quad \text{in} \qquad (2.16)$$

In calculating average eddy current for cradled configuration, S is taken equal to the axial spacing between conductors. Equations 2.19 also applies to the eddy current losses for single conductor cables which are installed in separate ducts.

2.7 Miscellaneous Components

Power cables generally have numerous metallic and non-metallic components used in their construction. These would include shielding tapes, metallic binder tapes, armor, skid wire, concentric neutral, jute covering and steel pipes. However, the author has restricted the discussion to paper insulated lead covered cables which would have only the shielding

tapes and metallic binder tapes used in their construction.

The shielding tape, usually copper, is applied over the paper dielectric on individual conductors. It is designed to conduct heat away from "hot spots" on the cable efficiently. It also prevents the formation of voids between the lead sheath and dielectric, thus reducing electrical stress. It has little effect on increasing the cable heat loss or adding significatly to the thermal resistance circuit and, therefore, is usually ignored.

Metallic binder tape is applied over an assembly of multiple conductor cable. It binds the conductors together during manufacture. It is designed to relieve mechanical stress on the lead sheath, particularly during power system faults when increased conductor currents would produce increased magnetic coupling between conductors. Binder tapes have a high thermal conductivity, cause only small increases in eddy and circulating current, and therefore, are also ignored in the cable ampacity calculations.

CHAPTER 3

THE THERMAL PROPERTIES OF THE CABLE SYSTEM

3.0 Introduction

Determining the thermal resistance of a multi-ducted bank as shown in figure 3.1 is not a simple problem. The physical construction of the duct bank, position of cables in the duct bank, some ducts being occupied while others not, and all the various thermal properties must all be considered. Because of the complexities for evaluating the earth path resistance mathematically, a solution using standard duct heating constants was developed in the 1930's by the National Electric Light Association (8).

The duct heating constants were based on average conditions and were not intended to account for variations in duct bank geometry, depth of burial below the surface, thermal resistivities, and so forth, factors which are different for every situation.

In 1949 Neher (10, 11) published two papers which presented a mathematical basis for calculating the relative thermal resistances from various duct positions to earth. The method was based on a number of approximations, but still provided reasonable results that allowed differentiation between the temperature rises of different ducts in a bank. The procedures developed by Neher have been modified over the past thirty years, but they are still the foundation for calculating cable ampacities analytically.

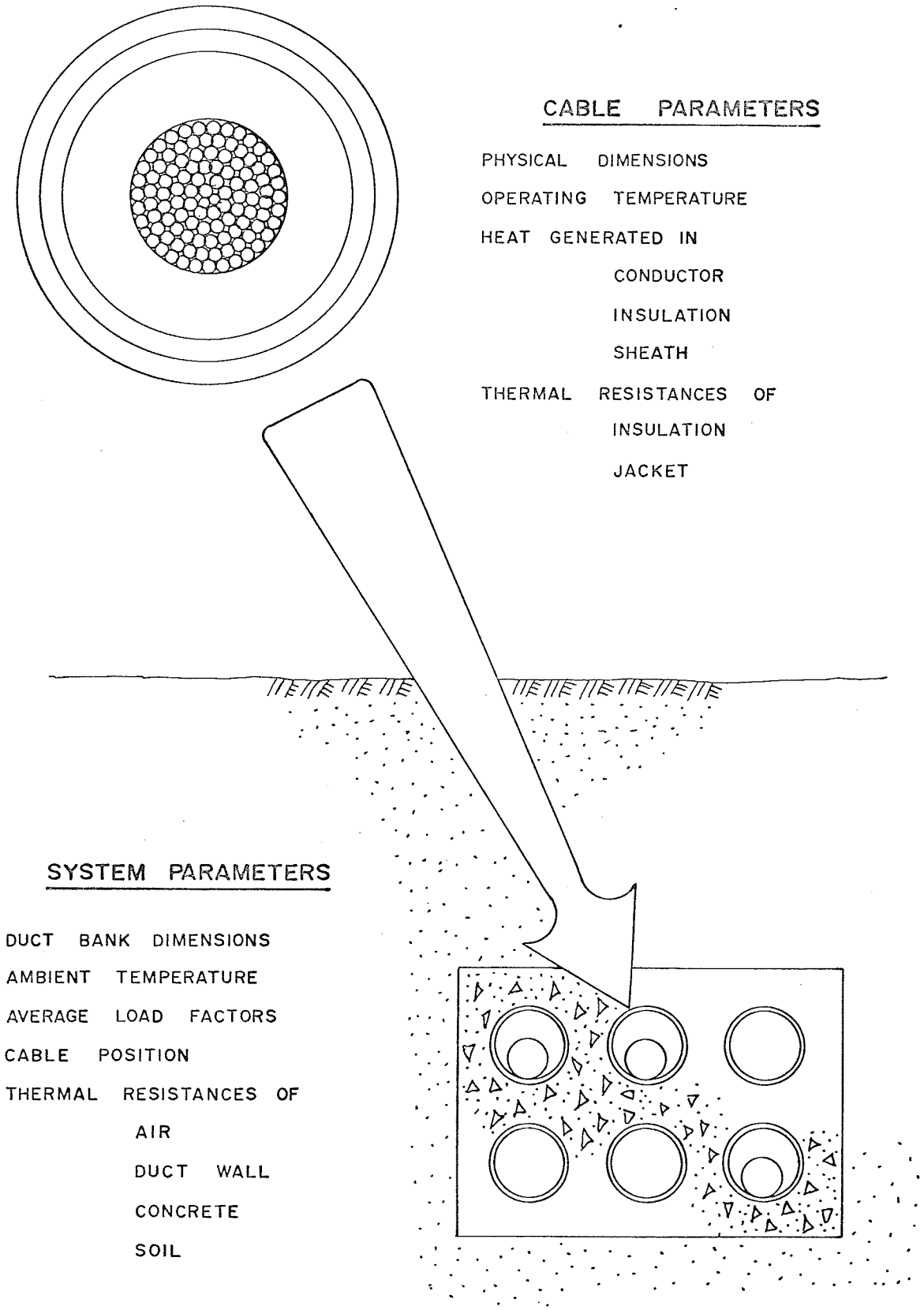

Figure 3.1 - PARAMETERS FOR A DUCT BANK SYSTEM

This chapter develops a procedure for calculating the thermal resistances from the ducts to ambient earth based on Neher's equations and those of others.

3.1 The Heat Transfer Equation

Heat transfer in underground power cable systems is generally analyzed in terms of conduction.

Heat by conduction is based on the property of a material to allow the passage of heat, even if the material is impermeable to any radiation and has no moving matter. The flow of heat is in a "steady state condition" if it is independent of time.

The fundamental relationship for the steady flow of heat by conduction as illustrated in figure 3.2(a) originates from the French physicists Biot and Fourier and is expressed by;

$$q = \frac{A}{\bar{\rho}} \frac{\Delta T}{\Delta X} \quad W \tag{3.1}$$

where q is the rate of heat flow in the direction of decreasing temperature, $\bar{\rho}$ is thermal resistivity of the material through which the heat passes, and ΔT is the constant temperature difference between a plane with an area A and a point P at a perpendicular distance ΔX from this area.

By applying this equation to a cylindrial section of insulation surrounding a conductor, as shown in figure 3.2(b), the rate of heat energy which flows radially through a differential volume of length l is expressed as (see Appendix A2)

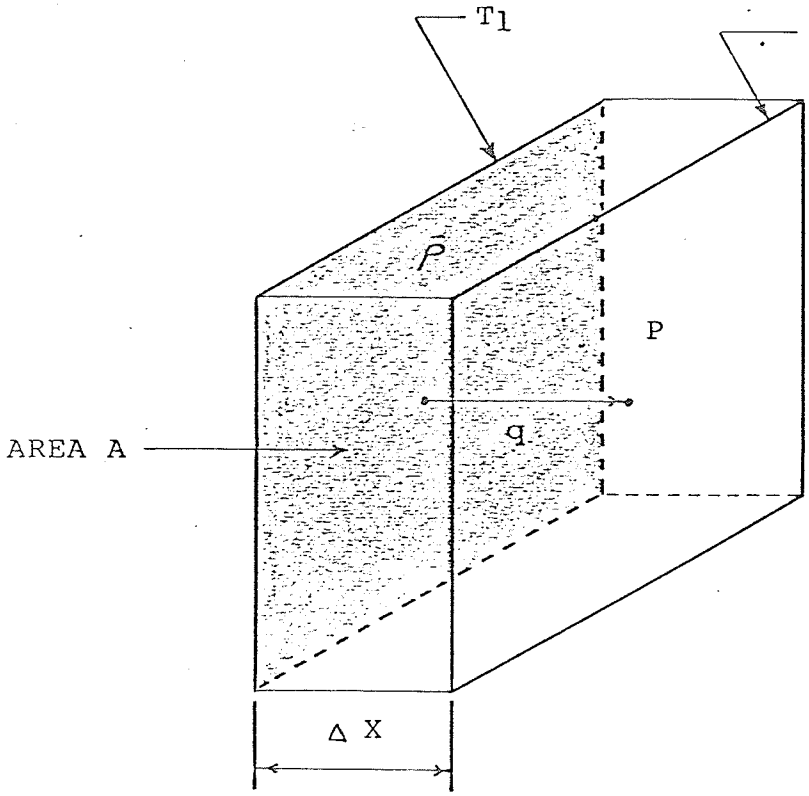

FIGURE 3.2(a) - HEAT CONDUCTION THROUGH A HOMOGENEOUS PLANE WALL

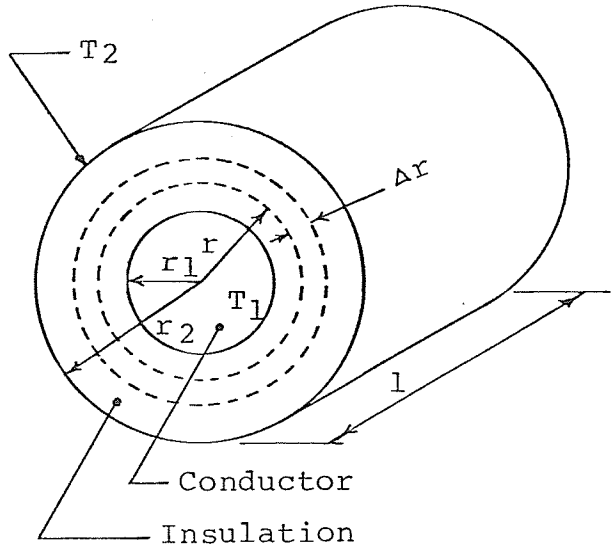

FIGURE 3.2(b) - HEAT CONDUCTION THROUGH A HOMOGENEOUS CYLINDRICAL WALL

$$Q = \frac{q}{l} = - \frac{2\pi r}{\bar{\rho}} \frac{dt}{dr} \quad W/ft \qquad (3.2)$$

Solving equation 3.2, the temperature difference between the two surfaces is;

$$\Delta T = \frac{Q\bar{\rho}}{2\pi} \ln \left[\frac{r_2}{r_1}\right] \quad {}^{o}C \qquad (3.3)$$

Using "Ohms Law for heat transfer", which is directly analogous to Ohm's Law for electrical circuits, the temperature difference between two points is equal to the product of the thermal resistance between the two points and the heat flow passing through (8).
Expressed mathematically,

$$\Delta T = Q \quad \bar{R} \quad {}^{o}C \qquad (3.4)$$

where

$$\bar{R} = \frac{\bar{\rho}}{2\pi} \ln \left[\frac{r_2}{r_1}\right] \quad {}^{o}C \text{ cm/W} \qquad (3.5)$$

The term $\ln \left[r_2/r_1\right]$ involves the physical shape of the insulation and is commonly called the geometric factor G. Equation 3.4 can be rewritten to express the temperature rise in terms of the heat W_c generated in the cable conductor as:

$$\Delta T = W_c \quad \bar{R} \quad {}^{o}C \qquad (3.6)$$

and

$$\bar{R} = 0.00522\ \bar{\rho}\ G \quad {}^{o}C \text{ ft/W} \qquad (3.7)$$

3.2 Thermal Resistance of the Cable Insulation

The thermal resistance of the insulation, or dielectric for a single conductor cable is calculated by

equation 3.5 as

$$\bar{R}_i = 0.00522\ \bar{\rho}_i\ G_i \quad {}^{\circ}C\ ft/W \tag{3.8}$$

where

$$G_i = \ln\left[\frac{D_c + 2t_i}{D_c}\right] \tag{3.9}$$

Typical values for $\bar{\rho}$ are given in Table 3.1. Geometric factors for other types of cable construction may be found in the references listed at the end of this thesis.

Material	$\bar{\rho}$ °C cm/W
Paper - Solid Type	600-700
Varnished cloth	600
Paper-Low Pressure Oil Filled	500
Rubber	500
Polyethylene	400
Polyvinyl chloride	700
Jute protective covering	500
Fibre Duct	480
Transite Duct	200
Concrete	85
Earth - Typical only	90

Table 3.1 - THERMAL RESISTIVITIES OF VARIOUS MATERIALS

3.3 Thermal Resistance of the Cable Jacket

Again, applying equation 3.5, the thermal resistance of the cable jacket is expressed as

$$\bar{R}_j = 0.00522\ \bar{\rho}_j\ G_j \quad {}^{\circ}C\ ft/W \tag{3.10}$$

where

$$G_j = \ln \left[\frac{D_j}{D_j - 2\ t_j} \right] \qquad (3.11)$$

Jackets are used when cable protection from unusual service conditions are required. Typically, polyvinyl choloride is used as a jacket material with a thermal resistivity given in Table 3.1.

3.4 Thermal Resistance of Miscellaneous Cable Components

Cable components including binding tapes, armor, skid wires and the sheath have very small thermal resistances and therefore are ignored in the thermal circuit. Cable wrappings such as jute, asbestos and similar thermal tapes are used in manholes and cable termination stations to provide physical protection to the cable. These wrappings do impede the escape of heat from the cable and their effects are calculated by applying equation 3.5. Since cables installed in ducts are being discussed in this paper, the effects of cable wrappings are not considered in detail.

3.5 Thermal Resistance Between the Cable Surface and the Duct Wall

The thermal resistance of the air space between a cable surface and duct wall are calculated from theoretical and semiempirical expressions developed by Buller et al (26) and Greebler et al (27).

$$\frac{1}{\bar{R}_{sd}} = \frac{Q}{\Delta T} = \frac{0.092\ D_s^{3/4}\ \Delta T^{1/4}\ P^{1/2}}{1.39\ \ D_s/D_d} + \frac{0.0213}{\log_{10}[D_d/D_s]} + 0.102\ D_s \epsilon\ (1 + .1067\ T_m) \qquad (3.12)$$

It is assumed that heat is dissipated from the cable surface through an intervening medium of air to the inner surface of the duct by conduction, convection and radiation, and that no forced cooling exists.

By further assuming $\Delta T = 20^{o}$ C across the air space, and D_s is in the range of 1-4 inches for cable in duct, Neher et al (9) have reduced equation 3.12 to

$$\bar{R}_{sd} = \frac{A}{1 + (B + CT_m)\ D_s} \quad {}^{o}C\ ft/W \qquad (3.13)$$

where A, B and C are constants dependent on the type of installation, some of which are given in Table 3.2.

Condition	A	B	C
Cable in metal Conduit	17.0	3.6	0.029
Cable in Fibre Duct in Concrete	17.0	2.3	0.024
Cable in transite Duct in Concrete	17.0	2.9	0.029

Table 3.2 - DUCT BANK CONSTANTS

3.6 Thermal Resistance of the Duct Wall

By equation 3.5 the thermal resistance of the duct wall is

$$\bar{R}_w = 0.00522\ \bar{\rho}_w\ G_w \quad {}^{o}C\ ft/W \qquad (3.14)$$

where

$$G_w = \ln\left[\frac{D_w + 2\,t_w}{D_w}\right] \qquad (3.15)$$

Typical values for duct bank construction materials are given in Table 3.1

3.7 Thermal Resistance of a Rectangular Duct Bank

A rectangular duct bank, shown in figure 3.3 represents a complicated shape compared to the cyclindrical radiators considered previously. Rather than applying a complex procedure to analyze heat transfer in the duct bank, the duct bank is represented as an isothermal circle with a radius given by (Appendix A3)

$$r_b = \ln^{-1}\left[\frac{1}{2}\,\frac{X}{y}\left[\frac{4}{\pi} - \frac{X}{y}\right]\ln\left[1+\frac{y}{X}^2\right] + \left[\frac{X}{2}\right]\right] \text{ in} \qquad (3.16)$$

where X is the smaller dimension and y is the larger dimension.

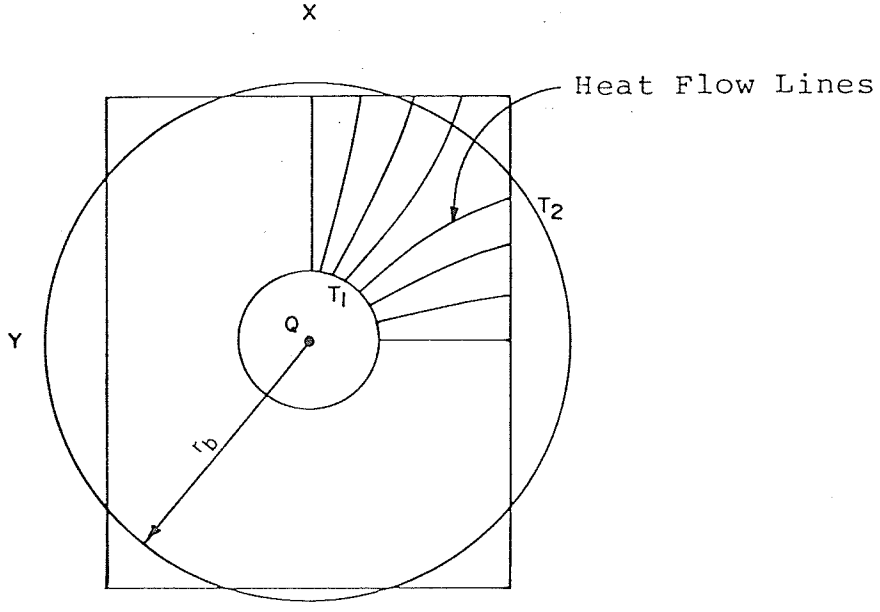

FIGURE 3.3 - HEAT FLOW LINES IN A RECTANGULAR DUCT BANK.

Applying equation 3.5, the thermal resistance of the duct bank is given by

$$\bar{R}_b' = 0.00522\ \bar{\rho}_b \ln\left[\frac{2\ r_b}{D_w + 2t_w}\right]\ ^{\circ}C\ ft/W \quad (3.17)$$

3.8 Thermal Resistance of Ambient Earth

The calculation of the thermal resistance between a duct bank and ambient earth are simplified by making several assumptions as follows:

i. the rectangular duct bank is represented as a cylindrical radiator as discussed in section 3.7

ii. the earth is initially at the same temperature throughout

iii. the earth has a constant thermal resistivity

iv. the heat generated in the duct bank in the steady state condition eventually finds its way to the earth's surface

v. the surface of the earth is treated as an isothermal surface.

Applying the method of images as discussed in Appendix A4, referring to figure 3.4, the temperature rise at any point P is expressed as

$$\Delta T_p = Q_c \frac{\bar{\rho}}{2\pi} \ln\left[\frac{d}{d'}\right]\ ^{\circ}C \quad (3.18)$$

This equation may be rewritten in terms of the equivalent radius of a duct bank r_b and the depth of its centre L_b below the surface of the earth to express the

temperature rise on the surface of the duct bank as

$$\Delta T_s = Q_c \bar{R}_e \ ^oC \tag{3.19}$$

where the thermal resistance of the earth is given by

$$\bar{R}_e = 0.00522 \bar{\rho}_e \ln \left[\frac{L_b + \sqrt{L_b^2 - r_b^2}}{r_b} \right] ^oC \text{ ft/W} \tag{3.20}$$

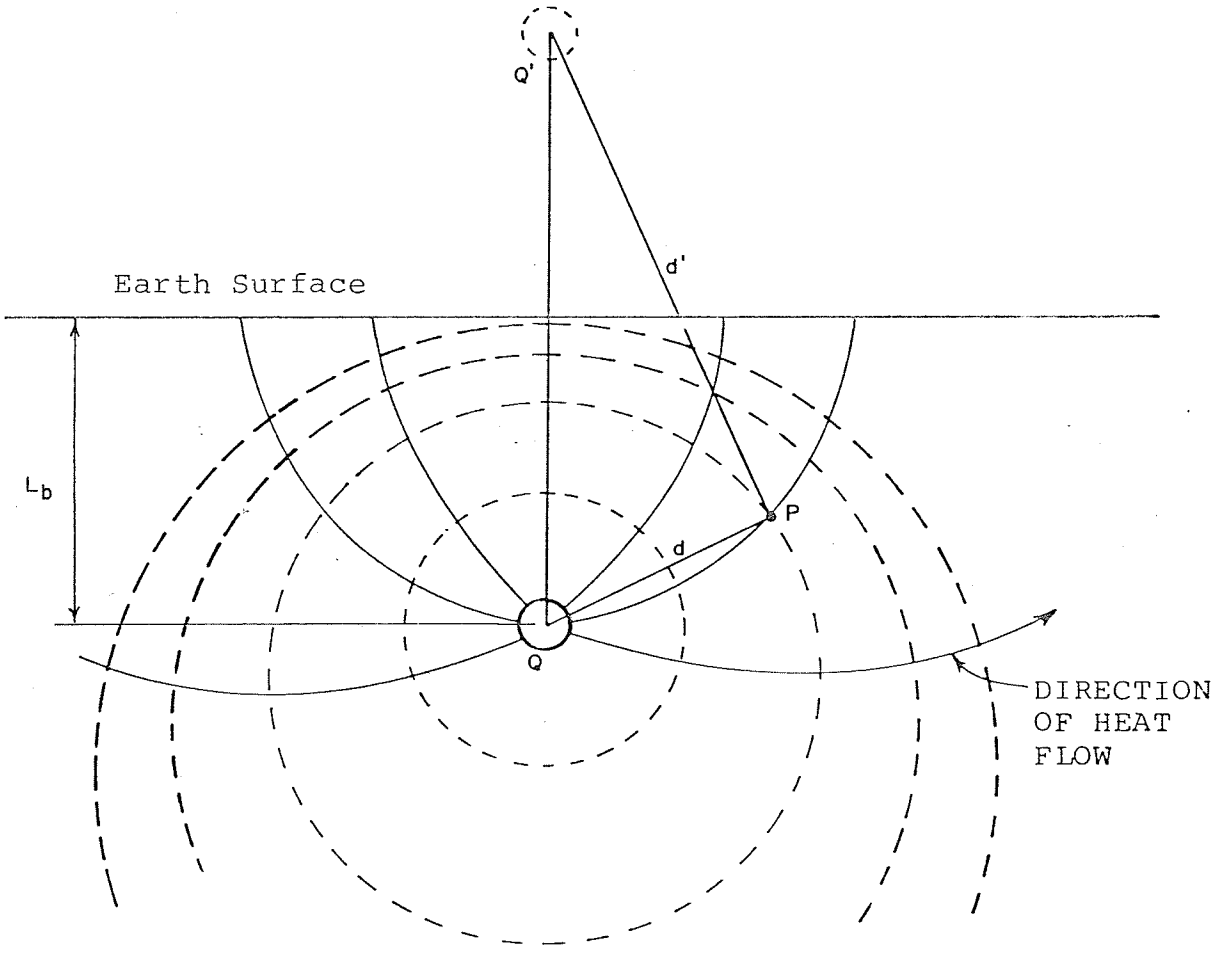

FIGURE 3.4 - HEAT FLOW IN AMBIENT EARTH

3.9 Loss Factor (12, 13, 14, 15)

A cable will conduct higher maximum current without exceeding a given conductor temperature if the load is cyclical rather than continuous. The thermal capacity of the cable and surrounding environment reduce the effect of load peaks on conductor temperature rise. Power cables usually have a definite daily load cycle, Figure 3.5, upon which longer load cycles such as seasonal may be superimposed. The daily load factor is defined as the ratio of the average load over a designated period of time, say 24 hours, to the peak load occurring in that period (16).

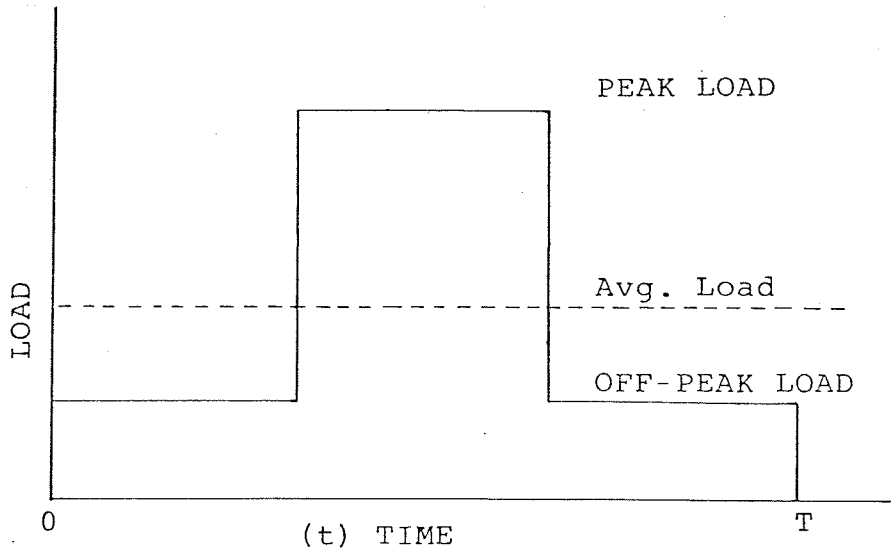

FIGURE 3.5 - CABLE LOAD CYCLE

The conductor losses in the cable will vary according to the cable load. A loss factor is applied to the cable losses to account for the cycling load. Manning (16) defines the loss factor as the ratio of the average power loss to the peak power loss during a specified time interval. The following empirical relationship between load factor F_{ld} and the loss factor F_{ls} is used for transmission and distribution systems:

$$F_{ls} = 0.3\ F_{ld} + 0.7\ (F_{ld})^2 \text{ p.u.} \qquad (3.21)$$

For a cable undergoing repeated daily load cycles, the losses and resultant heat flows are calculated on the basis of the maximum one hour average load. The loss factor is calculated and applied to the maximum load to average the losses over a 24 hour period.

It is generally assumed that the temperature of the cable and thermal circuit in the immediate proximity of the cable follow the load cycle closely, i.e., the thermal circuit temperature gradient will be exactly proportional to the loss variation. However, the thermal circuit farther from the cable reacts more slowly. If this delay in thermal response to load variation starts at a diameter D_x in the thermal circuit, the temperature rise from the conductor to D_x depends on the heat loss corresponding to the maximum load, whereas the temperature rise from diameter D_x to ambient earth depends on the average loss over a 24 hour period. The diameter D_x is expressed by Neher et al (9) for a sinusoidal load

cycle as

$$D_x = 1.02\sqrt{\alpha_e t} \quad \text{in} \tag{3.22}$$

Typically,

α_e = 2.75 in^2/hour for earth and,

t = 24 hours

Therefore,

$$D_x = 8.3 \text{ in} \tag{3.23}$$

The diameter D_x lies between the outside diameter of the duct wall $D_w + 2t_w$ and the equivalent diameter of the duct bank 2 r_b. Therefore, rewriting equation 3.17 as:

$$\bar{R}_b' = 0.00522\,\bar{\rho}_b \ln\left[\frac{D_x}{D_w + 2t_w}\right] + 0.00522\,\bar{\rho}_b \ln\left[\frac{2\,rb}{D_x}\right] \tag{3.24}$$

Letting

$$\bar{R}_{dx} = 0.00522\,\bar{\rho}_b \ln\left[\frac{D_x}{D_w + 2t_w}\right], \tag{3.25}$$

and

$$\bar{R}_b = 0.00522\,\bar{\rho}_b \ln\left[\frac{2rb}{D_x}\right], \tag{3.26}$$

$$\bar{R}_b' = \bar{R}_{dx} + \bar{R}_b \ ^{\circ}C \text{ ft/W} \tag{3.27}$$

The loss factor applies only to the conductor losses flowing through $\bar{R}_b$ and outward as shown in section 4.1.

CHAPTER 4

THERMAL CIRCUIT ANALYSIS

4.0 Introduction

This chapter combines the theories developed in chapters 2 and 3 to derive a system of equations which effectively describe the cable system. It is here that the author's handling of the cable system differs from the methods used by others. Simmons (8), Neher et al (9), and IPCEA (3) have developed their calculations based on the cable system having equally loaded identical cables. The cable ratings were based on selecting the hottest cable in the system configuration and limiting all the cables to this rating. However, these methods are not specific enough to analyze real situations where all the cables and loadings are not identical. The International Electro technical Commission (17) suggests that approximations be made to estimate the power dissipated in adjacent cables when calculating mutual heating effects of unequally loaded cables of different construction. Similarly Keyhani et al (18) developed equations for conductor current vs. inner conductor temperature for any given cable by an iteration technique to approximate mutual heating effects when solving a cable system for unknown conductor currents and temperatures.

The procedures discussed in this chapter develop a system of linear equations in terms of the unknown quantity for each cable, either conductor temperature or current,

so that an exact solution for these unknowns can be calculated directly.

4.1 The Steady State Heat Equation

The heat generated in the conductor, dielectric and sheath flows outward through the various thermal resistances and causes a temperature rise in each of the elements in its thermal path. The heat passes into the earth in all directions and is finally dissipated at the earth surface. A simplified diagram of the thermal path in terms of an electrical analogy is shown in figure 4.1.

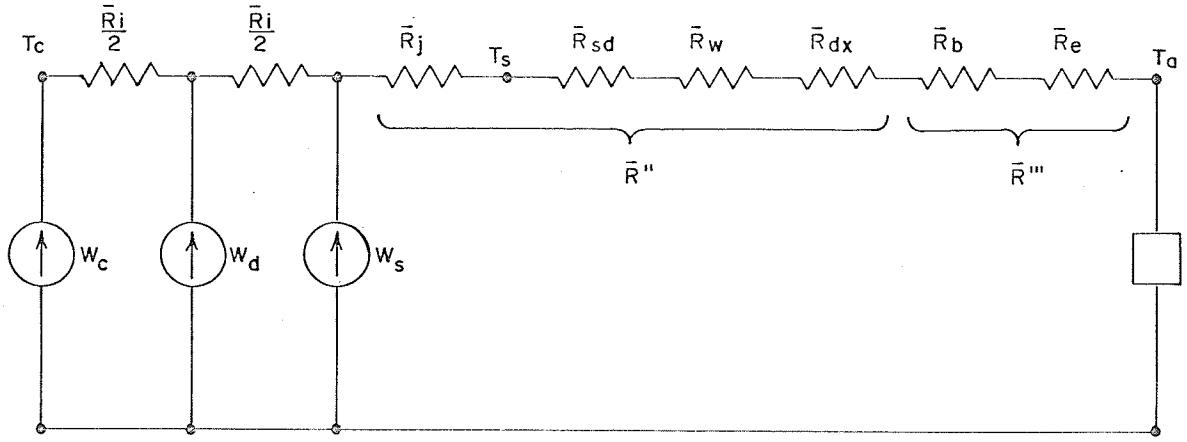

FIGURE 4.1 - ELECTRICAL ANALOGY OF THE THERMAL CIRCUIT

The effect of each source of heat loss, namely, the conductor I^2R loss W_c, the dielectric loss W_d and the sheath loss W_s, is analyzed separately and then the Superposition Theorem is applied to calculate the overall temperature rise of the conductor above ambient earth temperature.

4.1.1 Conductor Temperature Rise by I^2R Loss

The conductor loss W_c flows through the thermal resistances shown in figure 4.1. By equation 3.6, the temperature rise at the conductor surface is

$$\Delta T_c' = W_c \bar{R} \tag{3.6}$$

where

$$\bar{R} = \bar{R}_i + \bar{R}_j + \bar{R}_{sd} + \bar{R}_w + \bar{R}_{dx} + \bar{R}_b + \bar{R}_e \tag{4.1}$$

and

$$W_c = I^2 R_{ac} \frac{T + t_2}{T + t_1} \tag{2.10}$$

Assuming $T_c > T_a$,

$$\Delta T_c' = T_c - T_a = W_c \bar{R} \tag{4.2}$$

letting $R'_{ac} = R_{ac} \dfrac{T + t_2}{T + t_1}$ (4.3)

$$\bar{R}'' = \bar{R}_j + \bar{R}_{sd} + \bar{R}_w + \bar{R}_{dx} \tag{4.4}$$

and $$\bar{R}''' = \bar{R}_b + \bar{R}_e \tag{4.5}$$

Therefore, equation 4.2 becomes:

$$\Delta T'_c = T_c - T_a = I^2 R'_{ac} (\bar{R}_i + \bar{R}'' + \bar{R}''') \qquad (4.6)$$

To account for the cyclic nature of the conductor current, the conductor loss flowing through $\bar{R}''$ is multiplied by a loss factor F_{ls} as discussed in section 3.9.

Hence, the conductor temperature rise above ambient earth due to conductor heat loss is expressed as

$$\Delta T'_c = I^2 R'_{ac} (\bar{R}_i + \bar{R}'' + F_{ls} \bar{R}''') \qquad (4.7)$$

4.1.2 Conductor Temperature Rise by Sheath Loss

By referring to figure 4.1 and assuming $T_c > T_s > T_a$ the temperature rise ΔT_s at the sheath because of sheath loss is given by;

$$\Delta T_s = (W_{sc} + W_{se}) (\bar{R}'' + \bar{R}''') \qquad (4.8)$$

where W_{sc} and W_{se} are given by equations 2.17 and 2.19 respectively. Since the sheath currents are proportional to the conductor current, the loss factor also affects the temperature rise across R'' and, therefore,

$$\Delta T_s = (W_{sc} + W_{se}) (\bar{R}'' + F_{ls} \bar{R}''') \qquad (4.9)$$

For simplification, ΔT_s is assumed to be the temperature rise at the conductor caused by the sheath losses.

4.1.3 Conductor Temperature Rise by Dielectric Loss

The dielectric loss is assumed to be evenly distributed throughout the cable insulation. Therefore, to account for the temperature rise at the conductor due

to this loss, the temperature rise between the conductor and sheath is assumed to be half as much as if the loss was at the conductor.

$$\Delta T_d = W_d \left[\frac{\bar{R}_i}{2} + \bar{R}'' + \bar{R}''' \right] \qquad (4.10)$$

The dielectric loss is independent of load current and therefore no loss factor is applied.

4.1.4 Summary

By applying the Superposition theorem, the overall temperature rise between the conductor and ambient earth for single conductor cable is given by the summation of equation 4.7, 4.9 and 4.10, or

$$\Delta T_c = I^2 R'_{ac} \bar{R}' + \Delta T_d \qquad (4.11)$$

where,

$$\bar{R}' = \bar{R}_i + q \bar{R}'' + F_{ls} q \bar{R}''' , \qquad (4.12)$$

$$Ysc = \frac{1}{\bar{R}'_{dc}} \left[R_s \frac{X_m 2}{\sqrt{X_m 2 + R_s^2}} \right] , \qquad (4.13)$$

$$Yse = \frac{1}{R'_{dc}} \frac{3}{R_s} \left[\frac{D_{sm}}{2S} \right]^2 \left[\frac{f}{5.2} \right]^2 \left[1 + \frac{5}{12} \left[\frac{D_{sm}}{2S} \right]^2 \right] \qquad (4.14)$$

and

$$q = 1 + \frac{Ysc + Yse}{Yc} , \qquad (4.15)$$

4.2 Equations For a Multiple Duct System

Because of the complexity of equations required to describe a large duct system, a simple two duct system

is used to illustrate the principles involved in developing the equations. The equations are then written for a generalized duct system.

4.3 A Two Duct System

Consider a duct system where C1 and C2 represent single conductor cables in separate ducts. The temperature rise of C1 due to its own heat loss is determined by equation 4.11 as;

$$\Delta T_{11} = I_1^2 R_1' \bar{R}_1' + \Delta T_{d11} \qquad (4.16)$$

Similarily, the temperature rise of C2 is

$$\Delta T_{22} = I_2^2 R_2' \bar{R}_2' + \Delta T_{d22} \qquad (4.17)$$

In addition to the self heating, the temperature rise of C1 will also be affected by the heat interaction from C2. Expressions for the mutual heating between buried cables have been provided by Neher et al (9) and Neher (10,11). The temperature rise of C1 caused by the heating effect of C2 is expressed as

$$\Delta T_{12} = W_2 \bar{R}_{12} \qquad (4.18)$$

where $\bar{R}_{12}$ is the thermal resistance between C1 and C2, and W_2 is the heat loss from C2. By applying the Method of Images and assuming uniform thermal resistivities, for the duct bank and earth, the effective thermal resistance between any two cables is expressed as

$$\bar{R}_{12} = 0.00522\ \bar{\rho}_b \ln\left[\frac{d_{12}'}{d_{12}}\right] + 0.00522\ (\bar{\rho}_e - \bar{\rho}_b) \ln\left[\frac{2L_b}{r_b}\right] \qquad (4.19)$$

Expressing equation 4.18 in terms of the loss factor F_{1s} and using equation 4.15 to account for the cable sheath loss in C2, the temperature rise at C1 becomes

$$\Delta T_{12} = I_2^2 R_2' \bar{R}_{12}' + \Delta T_{d12} \qquad (4.20)$$

where

$$\bar{R}_{12}' = F_{1s_2} q_2 \bar{R}_{12}, \qquad (4.21)$$

and

$$\Delta T_{d12} = W_{d12} \bar{R}_{12} \qquad (4.22)$$

Similarily, the temperature rise at C2 caused by the mutual heating from C1 is

$$\Delta T_{21} = I_1^2 R_1' \bar{R}_{21}' + \Delta T_{d21} \qquad (4.23)$$

Now, applying the Superposition Theorem, the overall temperature rise of C1 is equal to the sum of temperature rises above ambient caused by all heat sources, or

$$\Delta T_1 = \Delta T_{11} + \Delta T_{12} \qquad (4.24)$$

and similarily,

$$\Delta T_2 = \Delta T_{21} + \Delta T_{22}$$

From equation 4.3, 4.16, 4.17, 4.20 and 4.23 and letting

$$a = \frac{T}{T + t}, \qquad (4.25)$$

$$b = \frac{1}{T + t}, \text{ and} \qquad (4.26)$$

$K_{11} = R_1 \bar{R}_1'$, $K_{12} = R_2 \bar{R}_{12}'$, $K_{21} = R_1 \bar{R}_{21}'$ and $K_{22} = R_2 \bar{R}_2'$, equation 4.24 becomes:

$$\Delta T_1 = I_1^2 K_{11}(a + b T_1) + \Delta T_{d11} + I_2^2 K_{12} (a + b T_2) + \Delta T_{d12}$$

$$\Delta T_2 = I_1^2 K_{21}(a + b T_1) + \Delta T_{d21} + I_2^2 K_{22} (a + b T_2) + \Delta T_{d22} \quad (4.27)$$

Since ΔT and ΔT_d are referenced to the ambient earth temperature T_a, and ΔT_d, independent of conductor temperature or current, is constant, equation 4.27 is rewritten as:

$$T_1 - T_a - \Delta T_{d11} - \Delta T_{d12} = I_1^2 K_{11} (a + b T_1) + I_2^2 K_{12} (a + b T_2)$$

$$T_2 - T_a - \Delta T_{d22} - \Delta T_{d22} = I_1^2 K_{21} (a + b T_1) + I_2^2 K_{22} (a + b T_2) \quad (4.28)$$

When analyzing a cable system, either the conductor temperature T or current I is known for each cable, and the other is calculated. Four conditions are available for the system being considered here. Each has a specific set of equations which is obtained from equation 4.28 as follows:

Condition 1: T_1 and T_2 known, I_1 and I_2 unknown.

$$T_1 - TA_1 = K_{11} (a + b T_1) I_1^2 + K_{12} (a + b T_2) I_2^2$$

$$T_2 - TA_2 = K_{21} (a + b T_1) I_1^2 + K_{22} (a + b T_2) I_2^2 \quad (4.29)$$

where,

$$TA_1 = T_a + \Delta T_{d11} + \Delta T_{d12}$$

$$TA_2 = T_a + \Delta T_{d21} + \Delta T_{d22} \quad (4.30)$$

Condition 2: I_1 and I_2 known, T_1 and T_2 unknown.

$$- TA_1 - I_1^2 K_{11}a - I_2^2 K_{12}a = (I_1^2 K_{11}b-1) T_1 + I_2^2 K_{12}b T_2$$

$$- TA_2 - I_1^2 K_{12}a - I_2^2 K_{22}a = I_1^2 K_{12}b T_1 + (I_2^2 K_{22} b-1) T_2 \quad (4.31)$$

Condition 3: I_1 and T_2 known; T_1 and I_2 unknown

$$- TA_1 - I_1^2 K_{11}a = (I_1^2 K_{11} b-1) T_1 + K_{12} (a + b T_1) I_2^2$$

$$T_2 - TA_2 - I_1^2 K_{12}a = I_1^2 K_{12} b T_1 + K_{22} (a + b T_1) I_2^2 \quad (4.32)$$

Condition 4: T_1 and I_2 known, I_1 and T_2 unknown.
- similar to condition 3.

The unknown temperatures and currents , for each condition are found by solving the appropriate set of homogenous linear equations.

Equation 4.29 may be expressed in matrix form as;

$$T = K \cdot I \quad (4.33)$$

where,

$$T = \begin{bmatrix} T_1 - TA_1 \\ \\ T_2 - TA_2 \end{bmatrix} \quad (4.34)$$

$$K = \begin{bmatrix} K_{11} (a + b T_1) & K_{12} (a + b T_2) \\ \\ K_{21} (a + b T_2) & K_{22} (a + b T_2) \end{bmatrix} \quad (4.35)$$

and,

$$I = \begin{bmatrix} I_1^2 \\ \\ I_2^2 \end{bmatrix} \quad (4.36)$$

Extending the discussion to a system of n cables, equations

4.34, 4.35 and 4.36 may be written as

$$T = \begin{bmatrix} T_1 - T_a - \Delta T_{d11} - \Delta T_{d12} - \cdots\cdots - \Delta T_{d1n} \\ T_2 - T_a - \Delta T_{d21} - \Delta T_{d22} - \cdots\cdots - \Delta T_{d2n} \\ \vdots \\ T_n - T_a - \Delta T_{dn1} - \Delta T_{dn2} - \cdots\cdots - \Delta T_{dnn} \end{bmatrix} \quad (4.37)$$

$$K = \begin{bmatrix} K_{11}(a + b\,T_1) & K_{12}(a + b\,T_2) & \cdots\cdots & K_{1n}(a + b\,T_n) \\ K_{21}(a + b\,T_1) & K_{22}(a + b\,T_2) & \cdots\cdots & K_{2n}(a + b\,T_n) \\ \vdots & & & \\ K_{n1}(a + b\,T_1) & K_{n2}(a + b\,T2) & \cdots\cdots & K_{nn}(a + b\,T_n) \end{bmatrix}$$

(4.38)

$$I = \begin{bmatrix} I_1^2 \\ I_2^2 \\ \vdots \\ I_n^2 \end{bmatrix} \quad (4.39)$$

Similar matrix sets may be developed for conditions 2, 3 and 4.

4.4 General Equations

As mentioned previously, either the current or operating temperature for each cable in a duct system is unknown. Therefore, letting **X** represent the unknown,

either I^2 or T, A represent the left hand side, and B represent thecoefficient matrix, a duct system containing n occupied positions is described by n equations. Expressed in matrix form

$$A = BX \tag{4.40}$$

More specifically,

$$\begin{aligned} a_1 &= b_{11}X_1 + b_{12}X_2 + \ldots\ldots\ldots\ldots b_{1n}X_n \\ a_2 &= b_{21}X_1 + b_{22}X_2 + \ldots\ldots\ldots\ldots b_{2n}X_n \\ &\vdots \\ an &= b_{n1}X_1 + b_{n2}X_2 + \ldots\ldots\ldots\ldots b_{nn}X_n \end{aligned} \tag{4.41}$$

This system of equations is solved for X_1, $X_2 \ldots X_n$, each representing either I^2 or T for each cable, and the particular ratings for the duct system are determined. One set of equations is developed for each duct bank configuration being studied. The coefficients b_{11}, b_{22}, etc. represent the thermal and electrical properties of the cable in each occupied duct position affected by self heating, whereas b_{12}, b_{13}, b_{21}, etc. represent the effects of mutual heating between occupied duct position.

CHAPTER 5

THE COMPUTER PROGRAM

5.0 Introduction

The computer program described herein permits the determination of the temperature or ampacity of a number of power cables in an underground duct system under steady state conditions. The analytical techniques developed in the previous chapters are programmed such that a cable system may be represented in terms of its various electrical and thermal characteristics. A direct solution is obtained for the unknown conductor temperature or current for each cable by solving the equations using the Gaussian Algorithm technique.

5.1 The Main Program; SLVCBL

Figure 5.1 shows a block diagram for the organization of the overall program. The blocks are described as follows:

i) Input/output handling blocks.

ii) A block which calculates the thermal resistances from the duct wall to ambient earth as discussed in Chapter 3.

iii) A block which calculates the electrical characteristics and thermal properties of the cable in each occupied duct as discussed in Chapters 2 and 3.

iv) A routine to calculate the coefficients for the system of equations which describe the specific cable config-

uration being analyzed.

v) A routine to solve the system of linear equations in terms of the known conductor temperatures and currents.

vi) A routine to calculate the unknown cable temperature or current for each occupied duct position.

vii) A block to calculate the temperature at the cable outer surface for each cable.

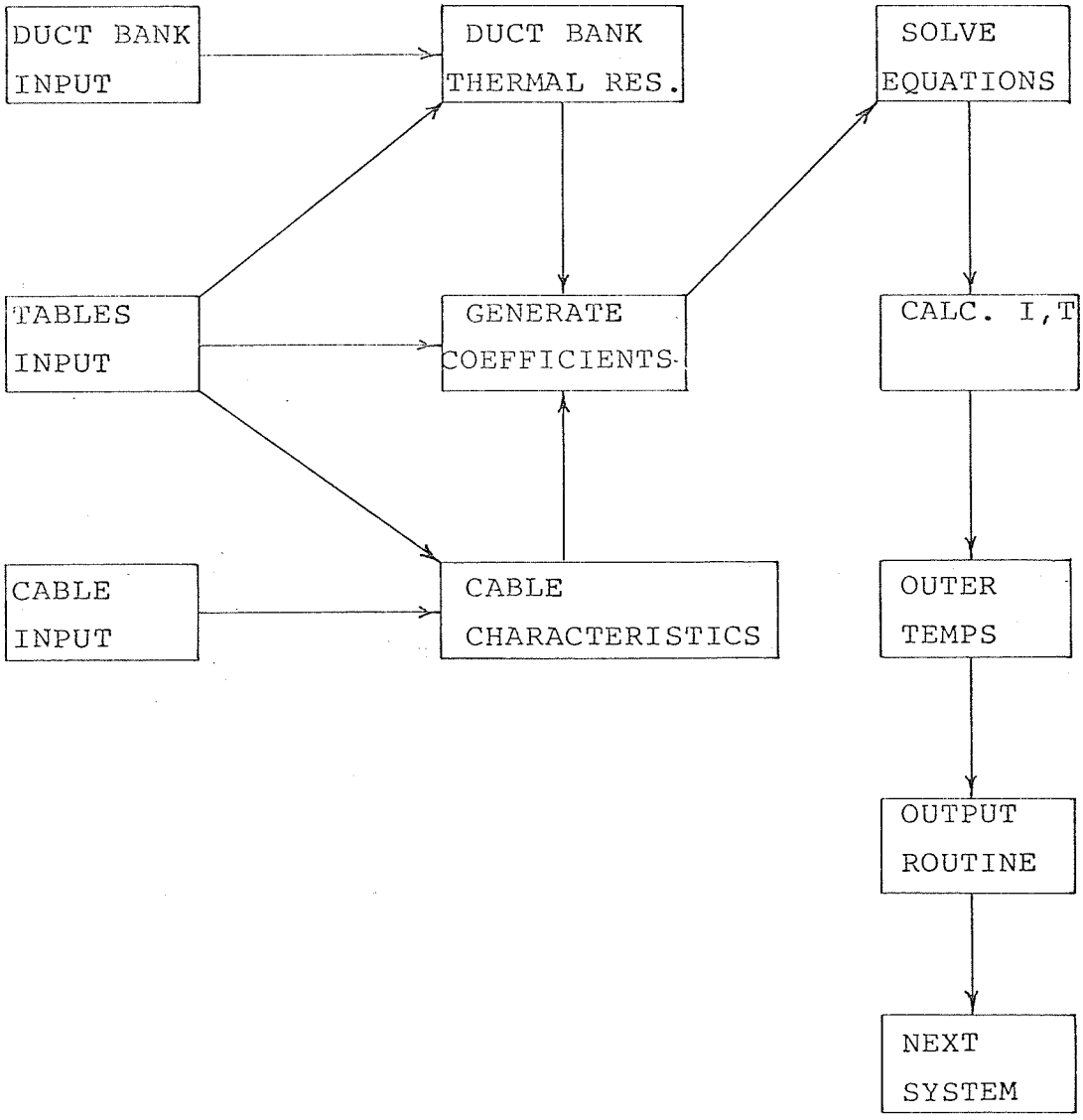

FIGURE 5.1 PROGRAM BLOCK ORGANIZATION

Figure 5.2 shows the flow chart for the program SLVCBL. This program controls the sequence for calling the various subprograms required to analyze the cable system.

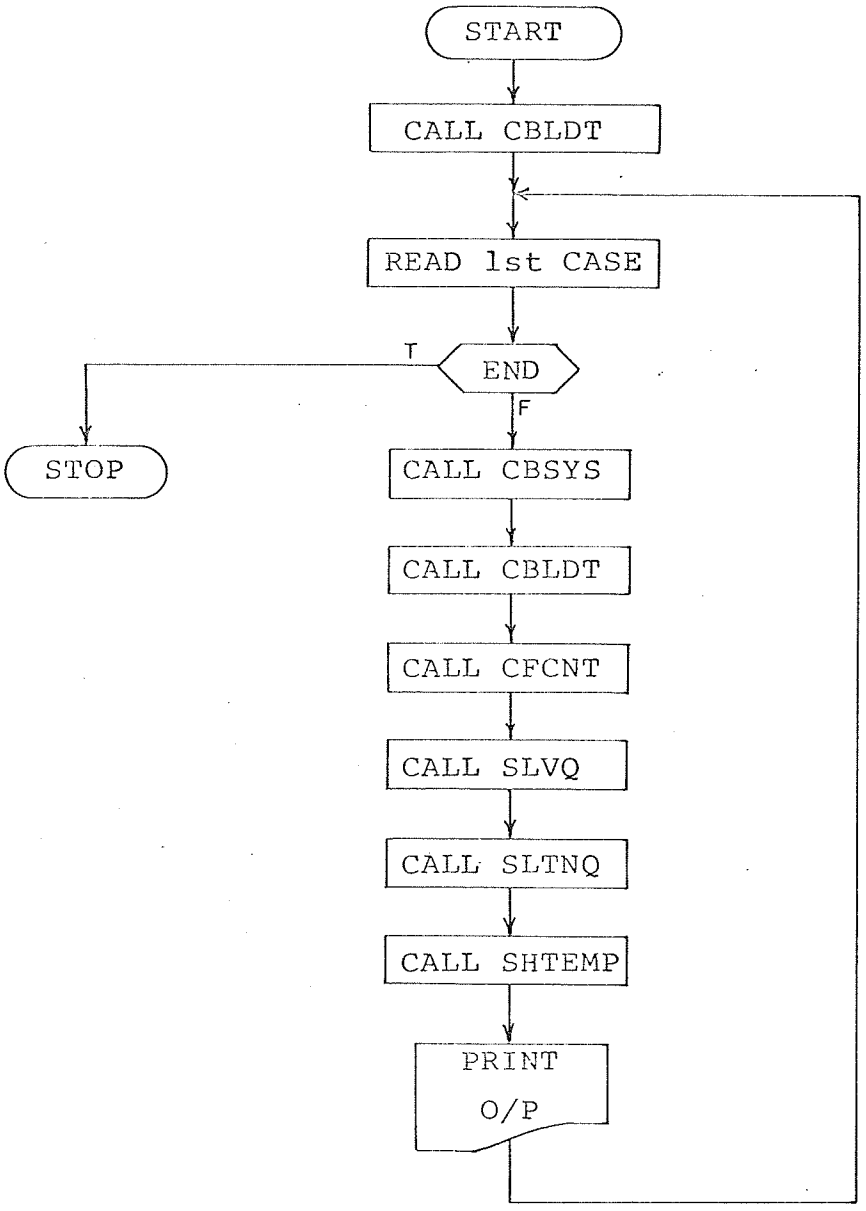

FIGURE 5.2 FLOWCHART FOR PROGRAM SLVCBL

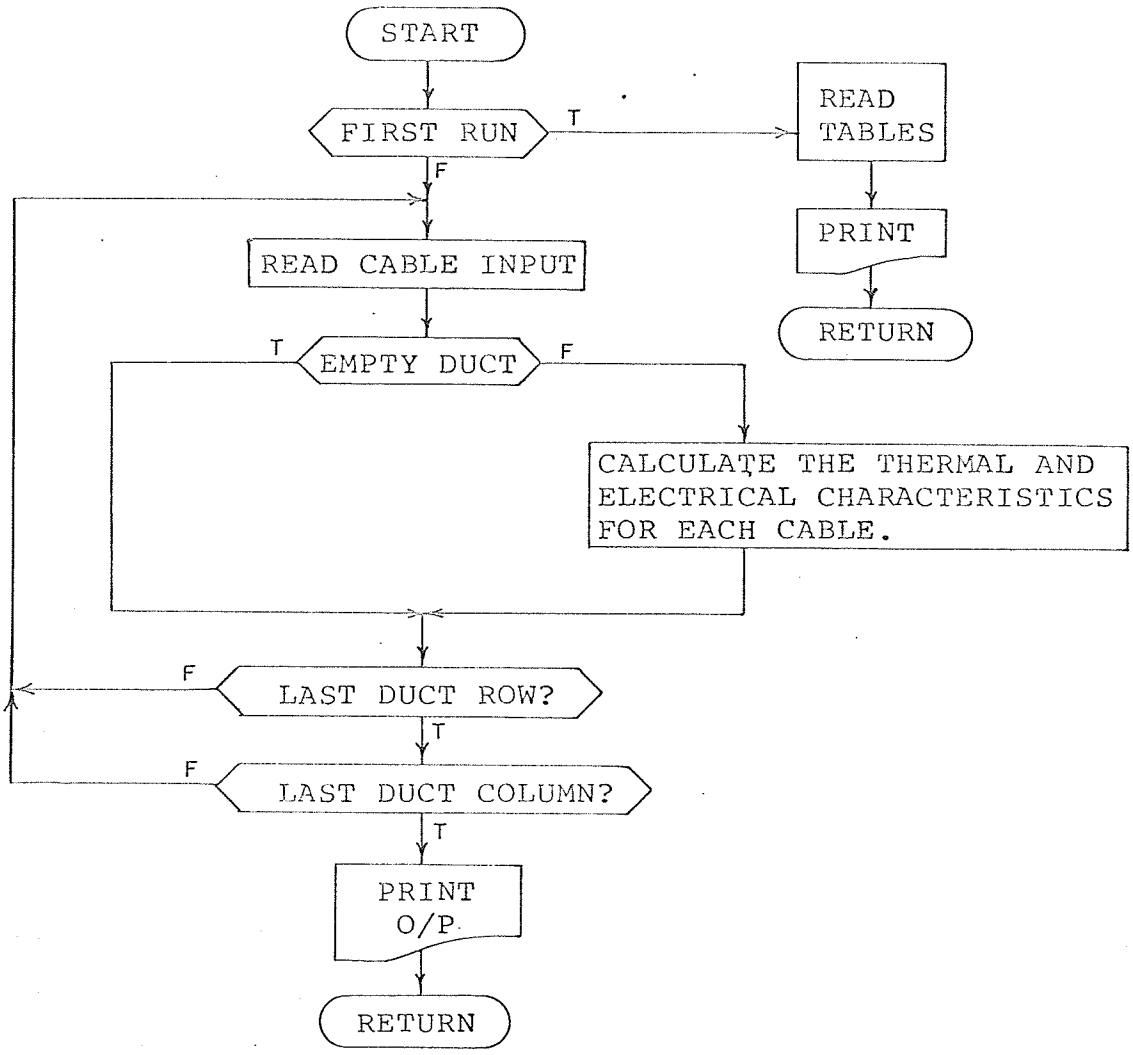

FIGURE 5.3 HIGH-LEVEL FLOWCHART FOR SUBPROGRAM CBLDT

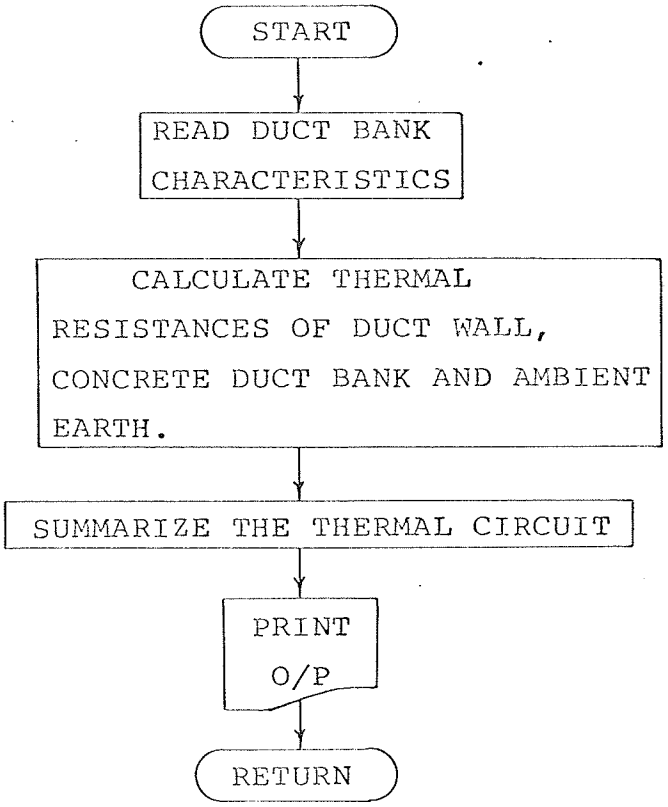

FIGURE 5.4 HIGH-LEVEL FLOW CHART FOR SUBPROGRAM CBSYS

5.2 The Subprograms

5.2.1 CBLDT

This subprogram reads the tables of data for cable characteristics, duct constants, and various cable configuration constants required during the course of calculations. This subprogram also calculates the thermal resistances between the conductor surface and the duct inner wall, the dielectric heat loss, the temperature rise caused by dielectric loss and the electrical resistance of the conductor and sheath for each cable in the duct bank. The equations developed in Chapter 2 and 3 are programmed into this routine. Figure 5.3 shows a high-level flow chart for this subprogram.

5.2.2 CBLSYS

The input data describing the physical and thermal properties of the duct bank are read, and the thermal resistances of the various thermal layers from the inner surface of a duct wall to ambient earth are calculated from the equation given in Chapter 3. Figure 5.4 shows the elementary flow chart.

5.2.3 CFCNT

This routine calculates the coefficients for the overall cable system equations. These coefficients, which are described in Section 4.2, include all the thermal and electrical properties of each cable in each

duct position as well as the thermal resistances to ambient earth. This program performs five tests before selecting the appropriate equations to calculate each coefficient for the general matrix described by equation 4.41. The duct positions are selected left to right, top to bottom as shown in figure 5.5

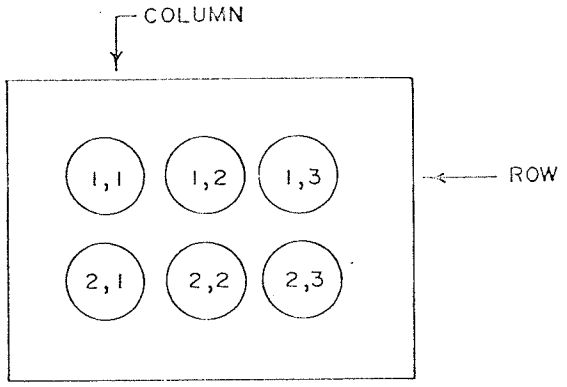

FIGURE 5.5 - SEQUENCE OF DUCT SELECTION

With reference to the high level flowchart shown in Figure 5.6 the following tests are made when calculating each coefficient:

1) A reference duct position is selected and tested for cable occupancy. If it is occupied, the program continues to the next test; otherwise, it is ignored

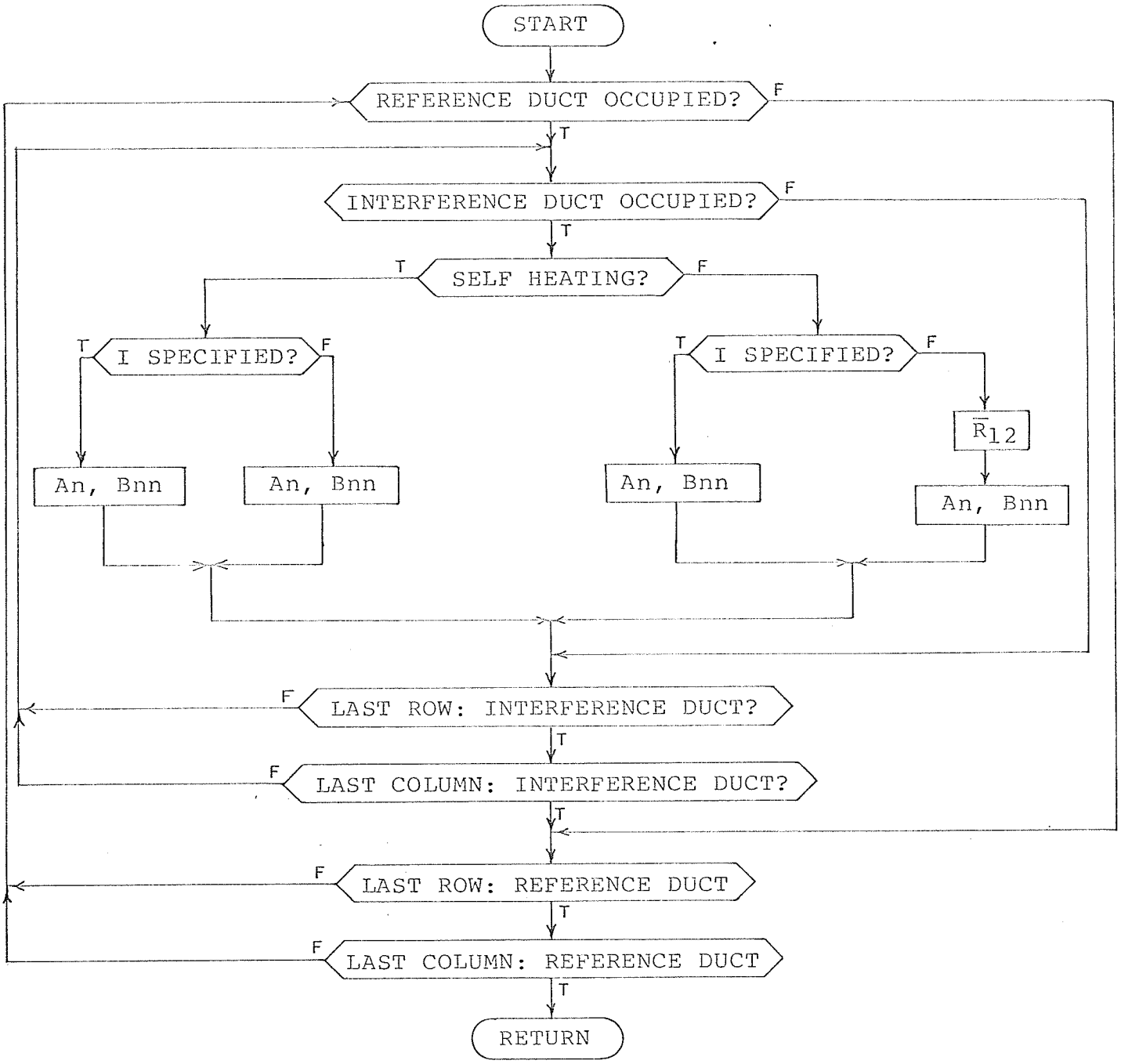

FIGURE 5.6 - HIGH LEVEL FLOWCHART FOR SUBPROGRAM CFCNT

and the next reference duct position is selected and tested.

2) An interference duct position is selected and tested. If it is unoccupied, it will have no affect on the reference cable position and it is ignored. If it is occupied, then the testing continues.

3) If the reference duct and interference duct position selected coincide, then they are in fact the same cable. Therefore, the heating at that duct position is calculated for self heating. If they do not coincide, then the mutual heating effect at the reference duct caused by the interference duct is calculated.

4) If the coefficient for self heating is being calculated in equation 4.41 and the conductor current is specified, then

$$A_n = A_n - T_a - T_d - aI^2 R_{ac} \bar{R}' \qquad (5.1)$$

where T_d, I^2, R_{ac} and $\bar{R}'$ are for the reference cable, and

$$B_{nn} = bI^2 R_{ac} \bar{R}' - 1.0 \qquad (5.2)$$

where I, R_{ac} and $\bar{R}'$ are also for the reference cable.

Similarily, if the conductor current is not specified, then

$$A_n = A_n + T - T_a - T_d \qquad (5.3)$$

where T and T_d are for the reference duct, and

$$B_{nn} = (a + bT) R_{ac} \bar{R}' \qquad (5.4)$$

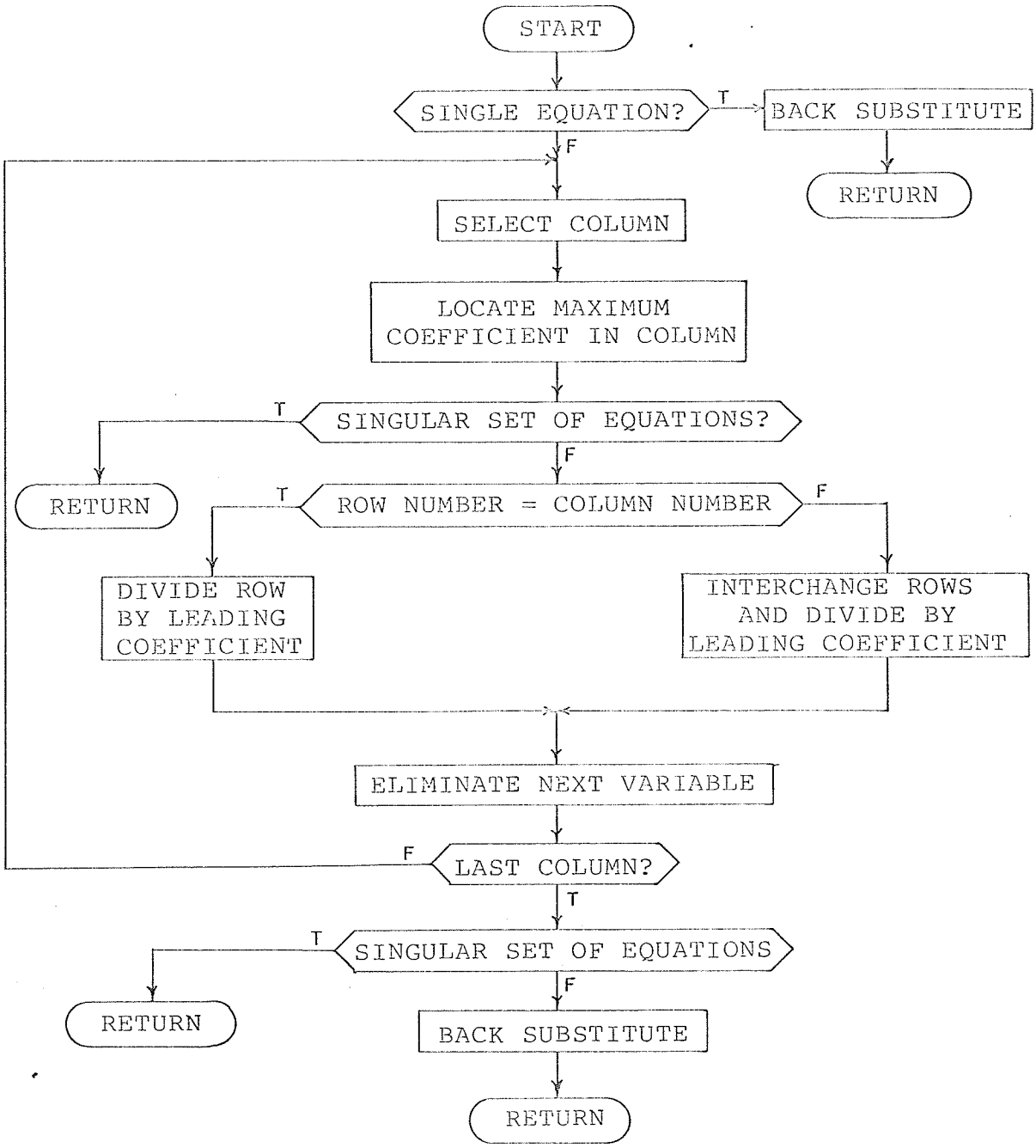

FIGURE 5.7 - HIGH LEVEL FLOWCHART FOR SUBPROGRAM SLVQ

where T, R_{ac} and $\bar{R}'$ are for the reference duct.

5) The coefficients for mutual heating are given as follows:

i. Current Specified;

$$A_n = A_n - aI^2 R_{ac} F_{ls} \bar{R}_{12} - W_d \bar{R}_{12} \qquad (5.5)$$

where I, R_{ac}, F_{ls} and W_d are for the interference cable position, and

$$B_{nn} = bI^2 R_{ac} F_{ls} \bar{R}_{12} \qquad (5.6)$$

where I, R_{ac} and F_{ls} are for the interference cable

ii) Current not specified;

$$A_n = A_n - W_d \bar{R}_{12} \qquad (5.7)$$

where W_d is for the interference cable, and

$$B_{nn} = (a + bT) R_{ac} F_{ls} \bar{R}_{12} \qquad (5.8)$$

where T, R_{ac} and F_{ls} are for the interference cable.

This sequence of tests and equations are repeated until the coefficient matrix is completed for all occupied duct positions.

5.2.4 SLVQ

This subprogram solves the system of equations in terms of known conductor temperature or current at each occupied duct position using the Gaussian Algorithm technique (19), (figure 5.7).

5.2.5 SLTNQ

This routine calculates the unknown conductor temperature or current for each cable from the output of SLVQ (figure 5.8)

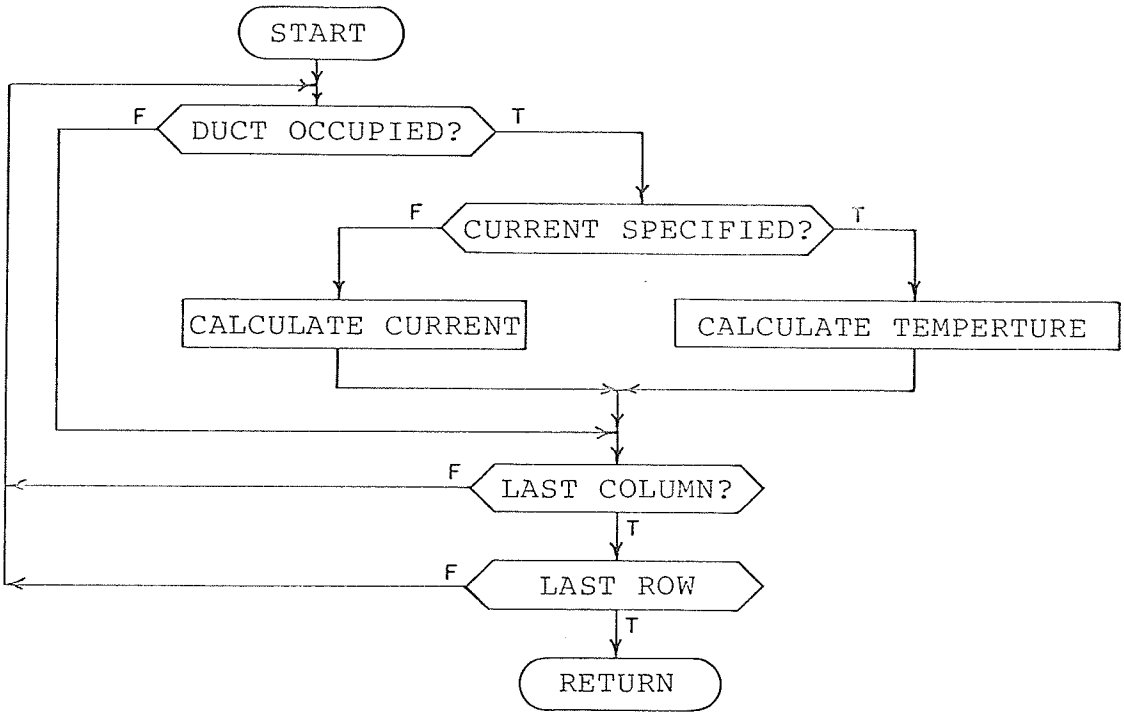

FIGURE 5.8 - HIGH LEVEL FLOWCHART FOR SUBPROGRAM SLTNQ

5.2.6 SHTEMP

The temperature of the conductor cannot be measured directly. However, monitoring the temperature of the cable outer surface provides a reasonable indication of cable thermal performance.

A routine is included in the program to calculate cable surface temperatures based on conductor temperatures and currents (figure 5.9). Measurements of actual cable

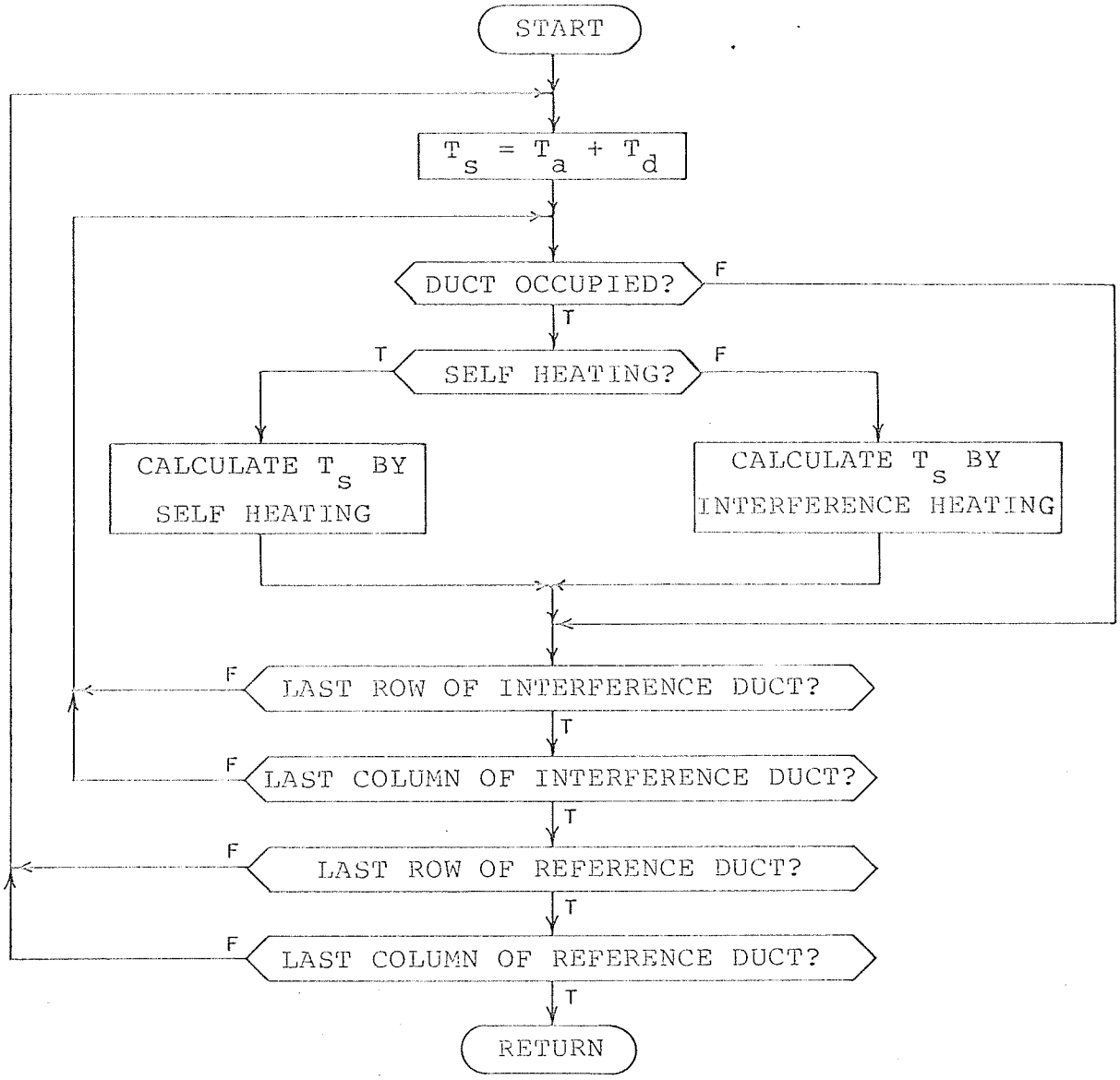

FIGURE 5.9 - HIGH LEVEL FLOWCHART FOR SUBPROGRAM SHTEMP

operating conditions may be taken, and read into the program to calculate the cable thermal permformance, including conductor surface temperatures. The calculated cable surface temperature may then be compared with actual measurements to varify results.

5.3 Summary

The flowcharts presented here are only high level flowcharts. For detailed flowcharts, program listings and user information on the program, the reader is referred to another technical report by the author (20).

CHAPTER 6

PROGRAM RESULTS AND DISCUSSION

6.0 Introduction

The ampacity ratings for cables are influenced by some parameters which are controlled and others which are not. The controlled parameters include selection of cable, physical construction of the duct bank and position of the cables in the duct bank. Parameters which are not controlled include earth thermal characteristics, ambient temperature variations, and characteristics of the load current itself.

This chapter discusses the effects of the various factors on cable ampacity. A 69 kV low pressure oil filled (LPOF) cable installed in a duct bank is analyzed and the results are shown graphically. Unless otherwise indicated, the following operating conditions apply:

i. conductor size: 850 MCM
ii. number of cables: six
iii. type of duct bank: two of three way
iv. depth: 30 inches to top of duct bank
v. cable spacing: 7.5 inches
vi. conductor temperature rating: 85^{o}C
vii. load factor: 1.0 p.u.
viii. earth thermal resistivity: 90^{o}C cm/watt
ix. ambient temperature: 20^{o}C

With all other conditions constant, each parameter is varied to determine its effect on cable ampacities.

While it is recognized that some of the situations discussed in this chapter are not practical, they are still included to illustrate the effect on cable current ratings.

Output from the computer program analysis is compared with IPCEA(3) cable rating tables and field measurement for a typical duct bank installation to verify the analytical calculation method presented in this thesis.

6.1 Controlled Cable System Parameters

6.1.1 Conductor Size

The heat loss produced in the conductor is a function of the load current and conductor resistance, which in turn is proportional to the conductor cross sectional area, or conductor size. Figure 6.1 illustrates the effect of conductor size on the ampacity rating for single conductor cables in a duct bank. For a given load requirement, say 1000 amperes, one circuit of 3-1500 MCM cables, or two circuits of 6-600 MCM cables are suitable. However, economics, reliability and physical constraints for duct bank construction influence the selection of the type of installation to be utilized.

6.1.2 Number of Cables In a Duct Bank

The ampacity of each cable is affected by the heat contribution of other cables in the system. The maximum current rating of each cable is reduced as the duct bank is required to dissipate more heat.

Each cable is operating at its continuous temperature

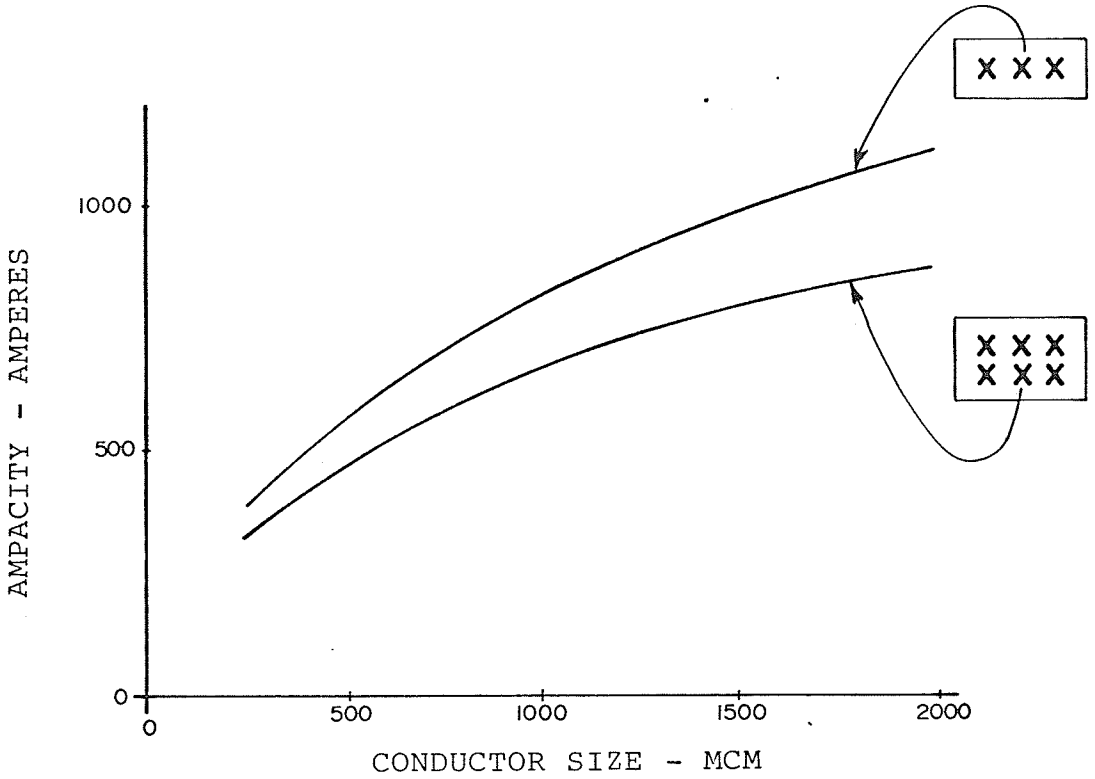

FIGURE 6.1 - EFFECT OF CONDUCTOR SIZE

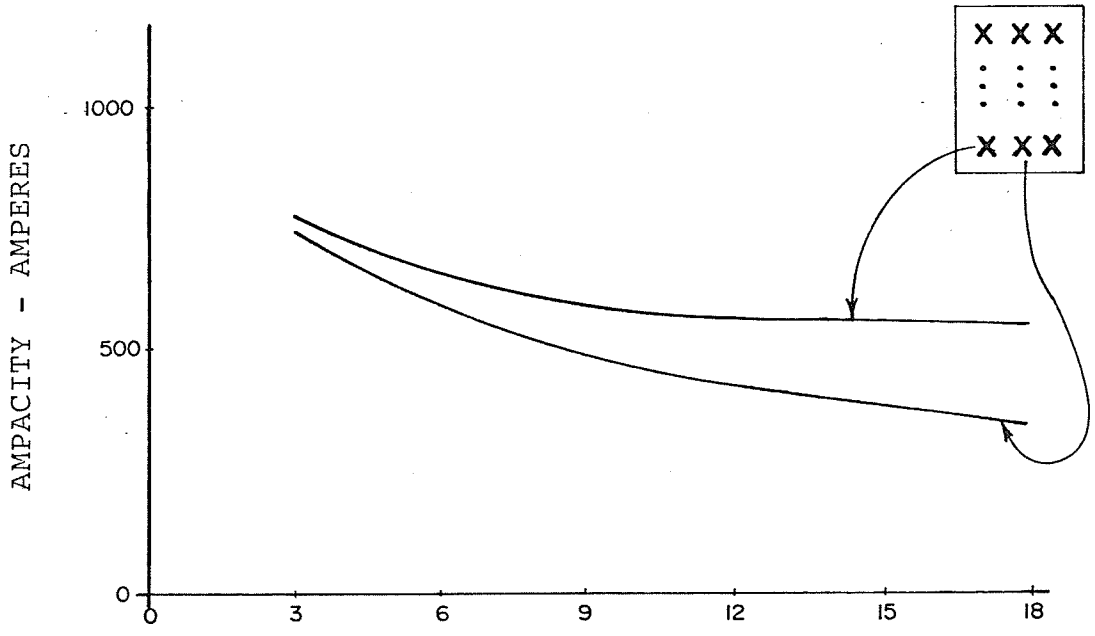

FIGURE 6.2 - EFFECT OF NUMBER OF CABLES IN A DUCT BANK

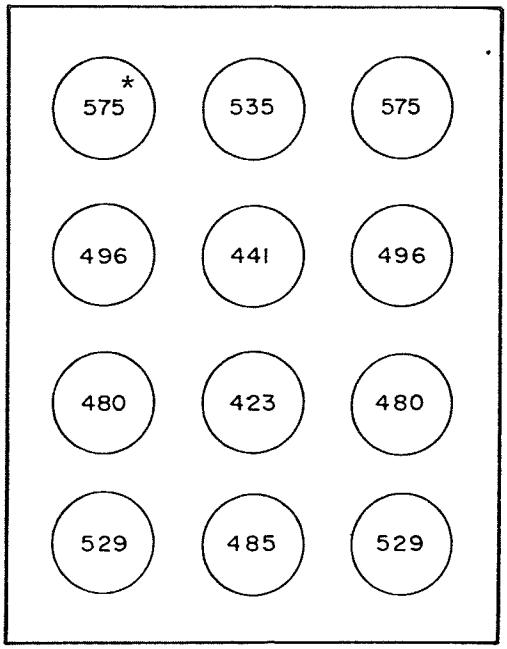

(a)

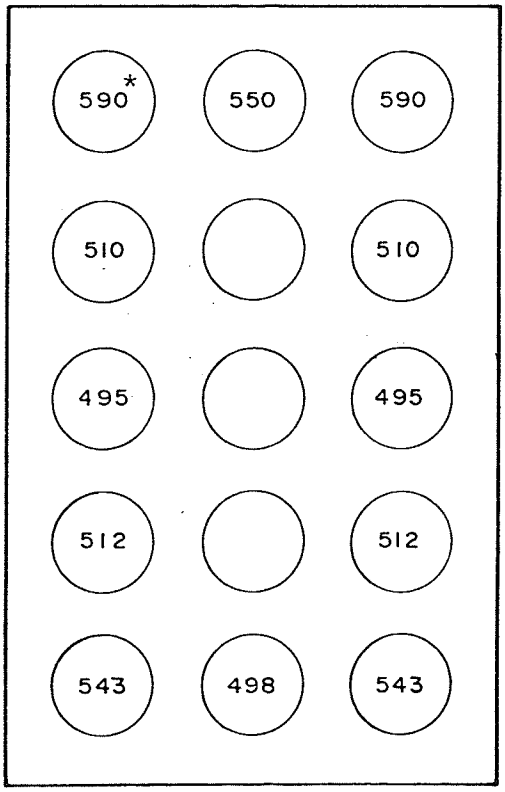

* Amperes

(b)

FIGURE 6.3 - EFFECT OF CABLE POSITION

limit (85°C) in figure 6.2. The range between the two curves represents the variation in ampacity for the cables, depending on their position in the duct bank. For a 12 cable system, and all conductors at 85°C, the ampacity ranges from a minimum of 423 amperes to a maximum of 575 amperes, depending on the cable position in the duct bank. Standard practices based on cable rating tables would limit the rating of all cables to 423 amperes, whereas one observes that some cables could carry higher currents without exceeding temperature limits. This is illustrated in more detail in the next section.

6.1.3 Cable position in a Duct Bank

It is desirable to have as many ducts as possible along the outer surface of the duct bank to facilitate heat dissipation to the surrounding earth. Figure 6.3(a) shows the effect of duct position on the ampacity of cables in a four of three way duct bank. Figure 6.3(b) gives the effect of placing the same number of cables around the perimeter of a larger duct bank. From this illustration one concludes that heavily loaded cables should be positioned around the perimeter of the duct bank to maximize cable ampacities and the inner ducts should be utilized for other purposes such as communication cables.

6.1.4 Spacing Between Ducts

The effect of varying the spacing for a two of three way duct bank on the cable ampacity is given in figure 6.4

Strictly speaking, the effect of increased duct spacing is not very significant, and is not practical when the increase in duct bank size required to achieve the spacing is considered. A typical spacing is 7.5 inches.

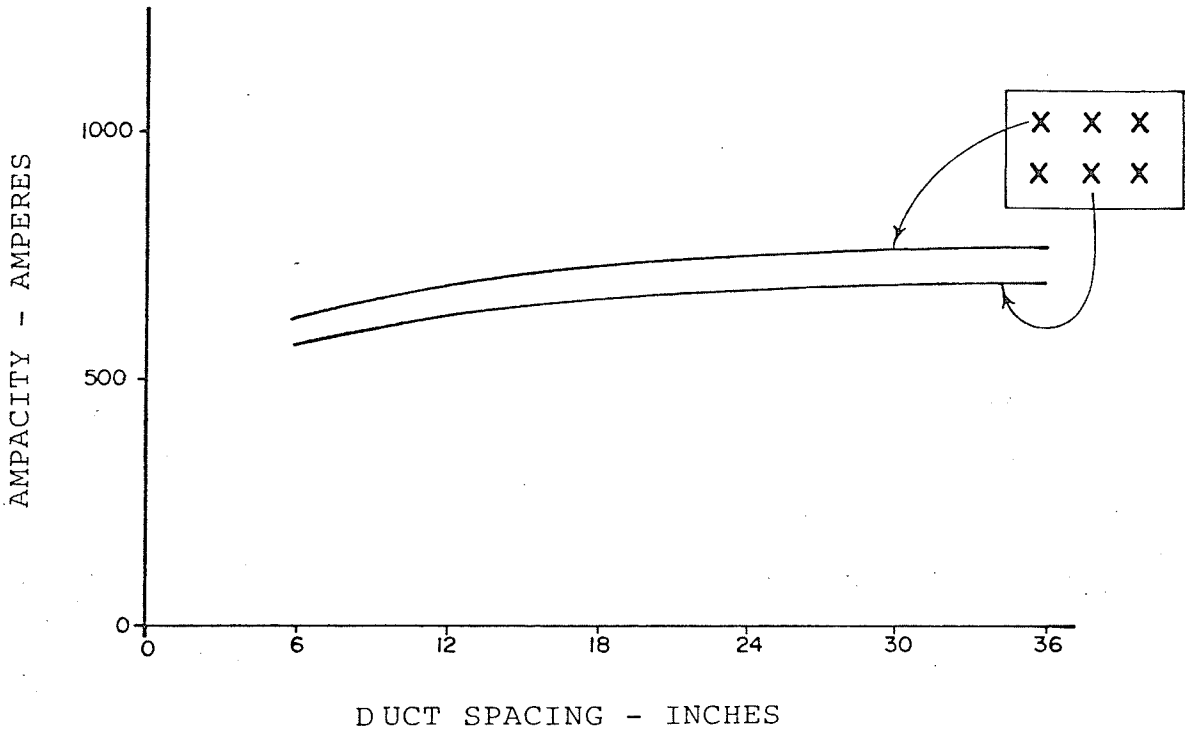

FIGURE 6.4 - EFFECT OF DUCT SPACING

6.1.5 Shape of A Duct Bank

By examining equations 3.16, 3.20 and 4.19, one would expect the resistance of the thermal circuit to be lower with an increase in duct bank equivalent radius r_b.

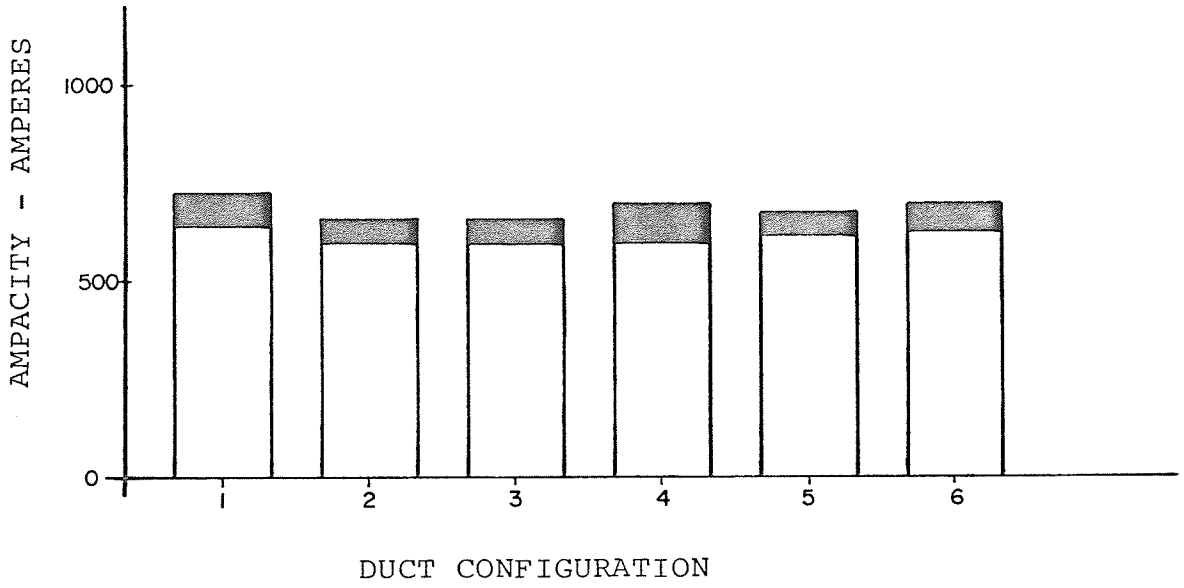

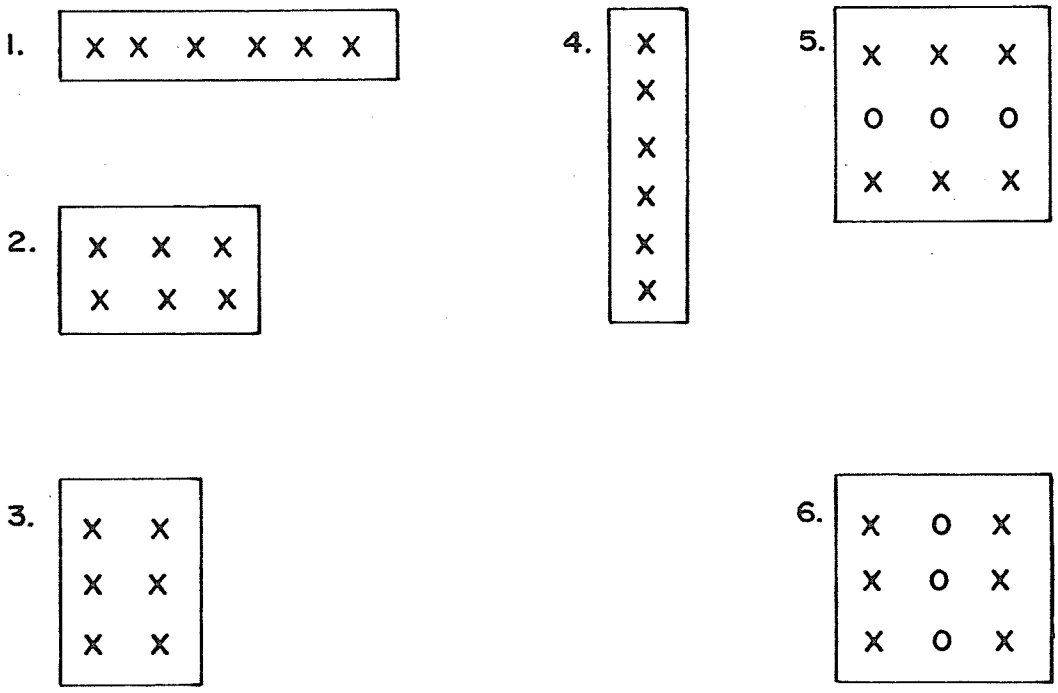

FIGURE 6.5 - EFFECT OF DUCT BANK SHAPE

Figure 6.5 illustrates the effect of varying the shape of the duct bank on the ampacity of a six cable system. The shaded area represents the range of cable currents, depending on position in the duct bank. Although configuration (1) and (4) result in higher conductor currents, they are usually not practical to construct. The remaining four configurations do not result in significant effects on the conductor ampacities.

6.1.6 Depth of A Duct Bank

The form of equations 3.20 and 4.19 indicate that thermal resistance in the duct bank system increases with increased depth. Figure 6.6 illustrates the effect of depth on the ampacity for two of three way duct bank with six cables. The effect of depth on cable ampacity becomes less significant as the depth increases beyond six feet. Typical depths are in the three to five foot range.

6.2 Variable Cable System Parameters

The cable system for a new installation is selected by making certain assumptions regarding the peak load currents to be carried, the load factor, ambient temperature and earth thermal characteristics. Conservative estimates are usually made to ensure the cables will have sufficient capacity to carry the load under the most severe operating conditions without exceeding conductor temperature limits. However, once the system has been installed,

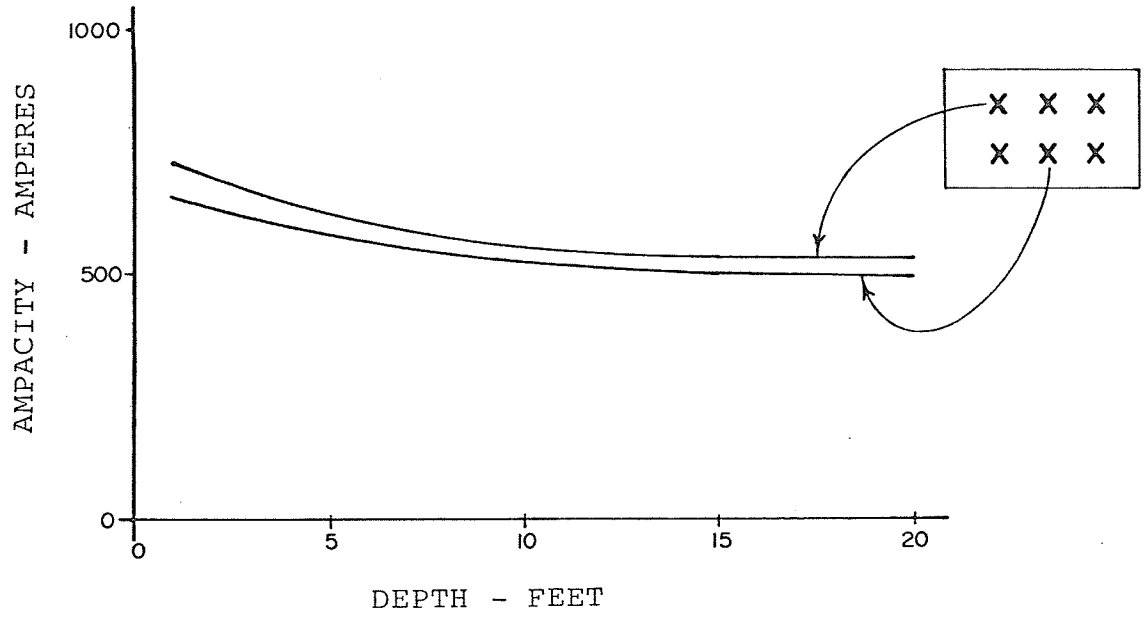

FIGURE 6.6 - EFFECT OF DEPTH

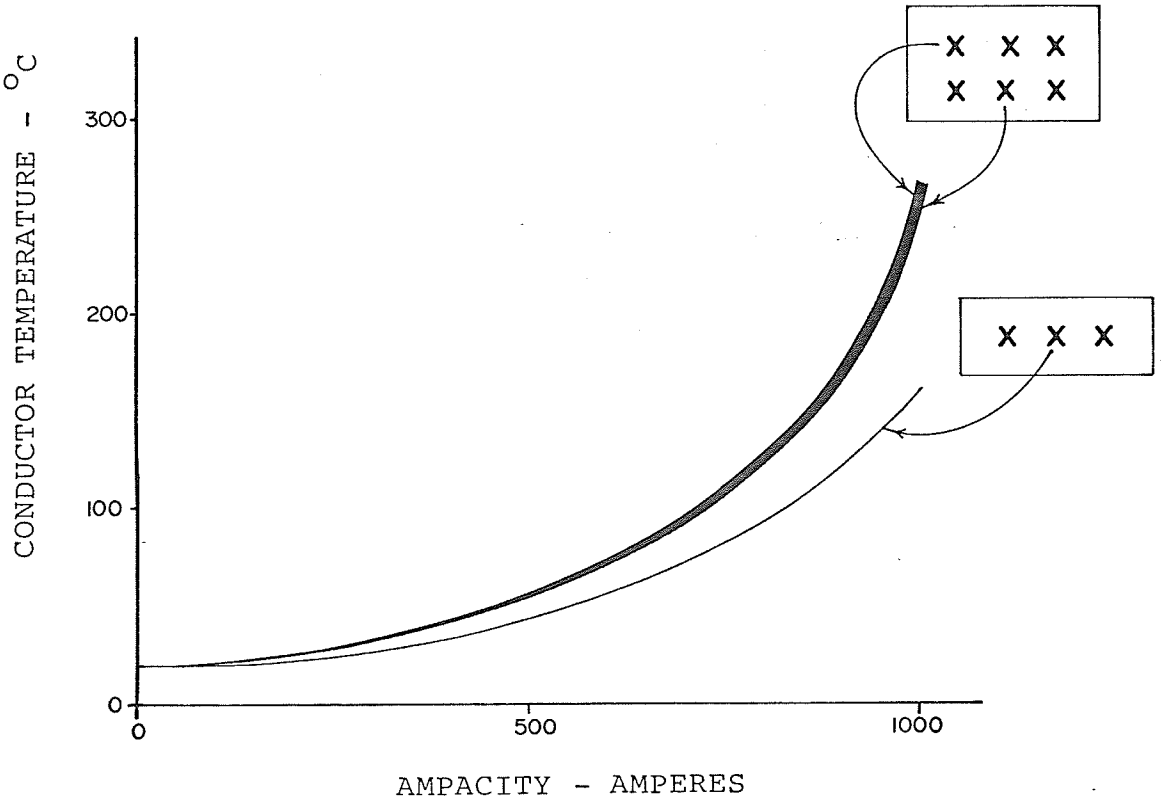

FIGURE 6.7 - EFFECT OF CONDUCTOR TEMPERATURE

tests may be performed to gain better insight into the actual operating performance of the cable system.

6.2.1 Peak Conductor Current

As discussed in section 3.9, the peak current is the maximum current carried by the cable over a particular 24 hour period. Measurements for a cable system may be made and the results may then be programed into the analysis to determine conductor operating temperatures (figure 6.7). Temperature limits for each type of cable are usually specified by the manufacturer. For example, the maximum continuous temperature rating for 69 kV low pressure oil filled cable is 85°C.

6.2.2 Load Factor

The effect of load factors on cable ampacities is shown in figure 6.8.

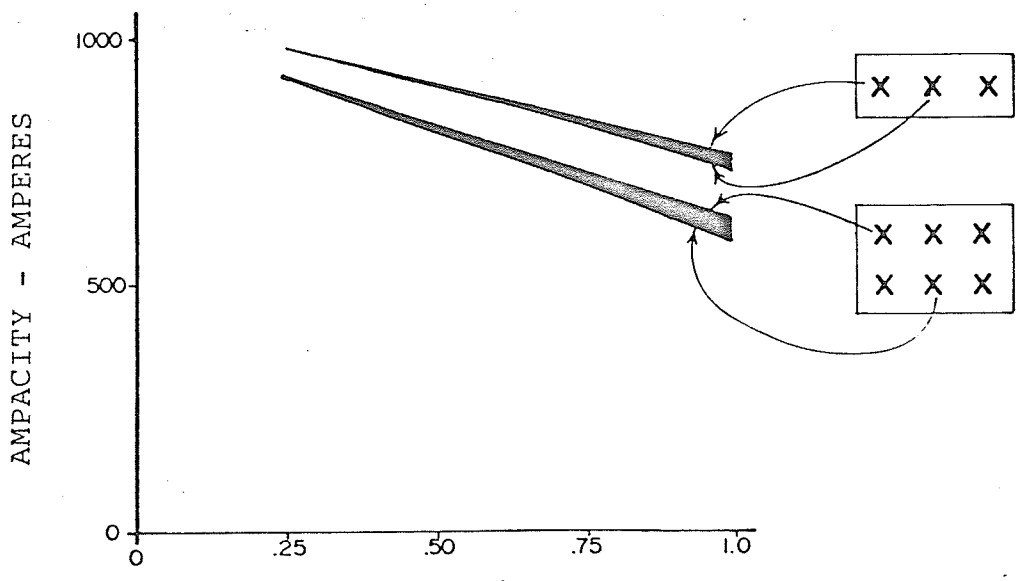

FIGURE 6.8 - EFFECT OF LOAD FACTOR

6.2.3 Ambient Earth Thermal Resistivity

Heat flows through the soil primarily by conduction from particle to particle. The heat transfer improves with more surface contact between particles due to their shape, amount of compactness and amount of moisture content in the soil.

Moisture content in the soil fills the gaps between soil particles and provides a "continuous" medium for effective thermal conduction. As the moisture is reduced below a "critical" moisture level, the bridging mechanism breaks down and the thermal resistivity increases dramatically. The soil structure and compactness determine the amount of moisture required to bridge the space between particles. Well graded soils such as limestone screenings maintain fairly constant thermal resistivities down to low moisture contents (2%) and are considered thermally stable while other soils such as clays have poor thermal stability even when saturated (20-30% moisture content). Soil moisture in most of North America varies on a seasonal basis (21). Precipitation input exceeds soil water use during cooler months while moisture deficiency and soil drying occurs during the hotter months.

Cable systems buried in semisaturated soil may experience a phenomenon called moisture migration. The soil moisture is driven away by the heat produced in the duct bank. The soil dries out and the soil thermal resistivity increases. J. B. Leach (22) suggests that

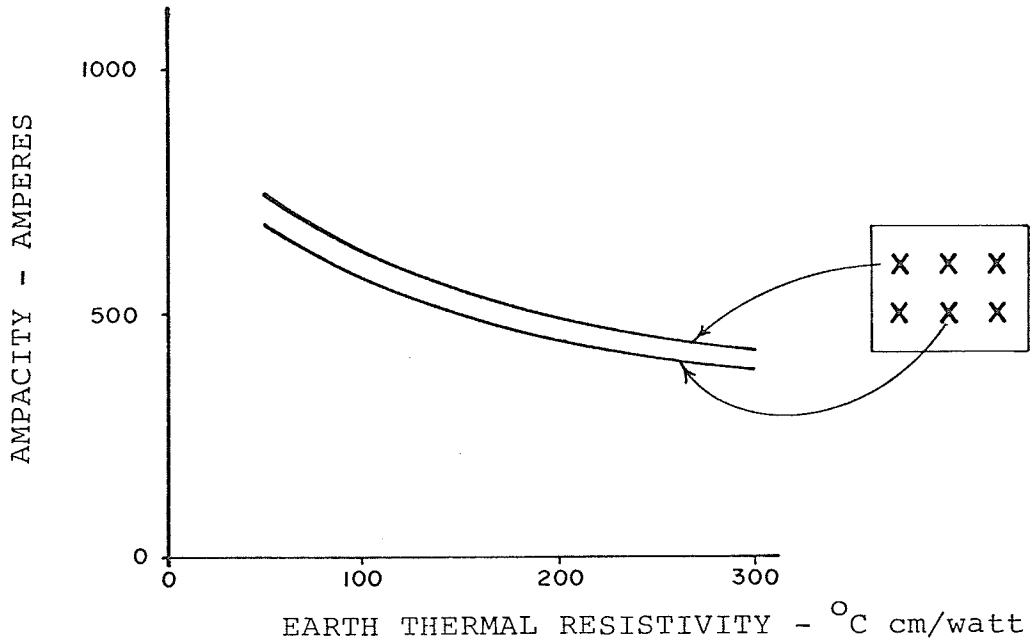

FIGURE 6.9 - EFFECT OF EARTH THERMAL RESISTIVITY

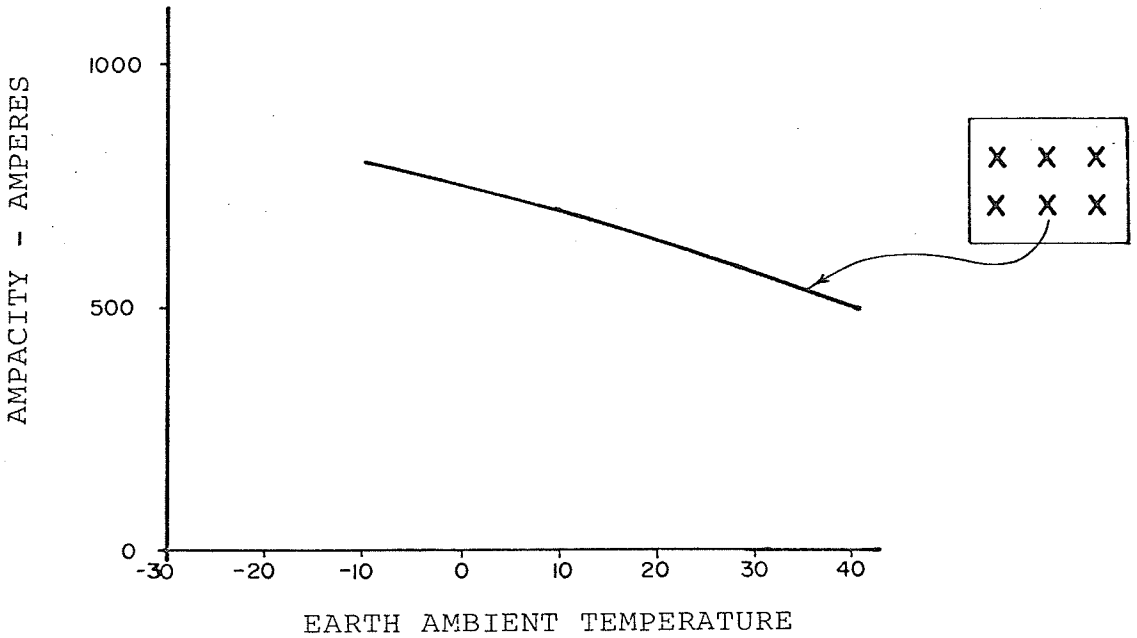

FIGURE 6.10 - EFFECT OF EARTH AMBIENT TEMPERATURE

an interface temperature between the concrete duct bank and earth exceeding 60°C is sufficient to drive the moisture away. The duct bank becomes thermally insulated and can result in thermal run-a-way.

The soil type, compactness and moisture content may vary along the same length of ductline. Therefore, conservative estimates for earth thermal resistivity should be used to represent the average-to-worst conditions along a duct line. Wherever practical, field measurements may be taken with devices such as a thermal needle (23, 24), or laboratory tests as discussed by Staple (25) may be made. Typical values of earth thermal resistivity range form 70°C cm/watt for average dry to 130 °C cm/watt for average wet conditions, but may be has high as 300°C cm/watt in extreme cases. When soil conditions are unknown, IPCEA(3) recommend using 90°C cm/watt.

Figure 6.9 shows the effect of earth thermal resistivity on cable ampacity for a typical two of three way duct system.

6.2.4 Ambient Earth Temperature

The soil temperature and its variation with seasons have a direct bearing on the heat dissipation from any heat source buried in the soil. As shown previously, the soil temperature enters into the calculation of the current capacity of buried cables.

The soil temperature near the ground surface is primarily a function of the thermal properties of the

soil as discussed in section 6.2.3, the heat transfer and moisture infiltration at the ground surface in the summer, and heat loss in the winter. Ground surface coverings such as pavement, sidewalks, grassy fields or snow also influence soil temperatures. Without going into detail, values of $0^{o}C$ for winter ambient and $20^{o}C$ for summer ambient are typical for cable analysis. However, measurements should be taken when more critical analysis is required.

Figure 6.10 illustrates the effects of earth ambient temperature variation on cable ampacity.

6.2.5 Extraneous Heat Sources

External heat sources such as steam mains, hot water pipes or other conduit systems affect the temperature rise of the duct system, but they are not considered in this thesis. They may be included in the analysis by using the principal of superposition and equation A4.10.

6.3 Correlation Between Computer Output and Existing Standards.

The ampacities calculated by the computer program for 850 MCM 69 kV low pressure oil filled cables in a 3 of 2 way duct bank are shown in Tables 6.1. Ampacities as recommended by IPCEA(3) are included in the table for comparison. IPCEA base the ampacity rating on the cable position with the lowest conductor current for a given conductor operating temperature, whereas the computer program calculates the current rating at each

cable position in the duct bank. This may not be important for single conductor cables, but it becomes more significant when rating three conductor cables or three single conductor cables in the same duct. The ampacities calculated agree favorably with the IPCEA(3) recommended ratings.

Fld / $\bar{\rho}_e$	CABLE POSITION	.50		.75		1.00	
		IPCEA	CALC.	IPCEA	CALC.	IPCEA	CALC.
60	1,1		886		798		718
"	1,2		886		798		718
"	2,1	866	860	763	756	674	660
"	2,2		860		756		660
"	3,1		875		781		695
"	3,2		875		781		695
90	1,1		836		734		647
"	1,2		836		734		647
"	2,1	812	811	698	695	605	594
"	2,2		811		695		594
"	3,1		825		718		626
"	3,2		825		718		626
120	1,1		793		682		593
"	1,2		793		682		593
"	2,1	765	769	646	646	555	545
"	2,2		769		646		545
"	3,1		783		667		574
"	3,2		783		667		574

TABLE 6.1 CORRELATION BETWEEN IPCEA AND COMPUTER OUTPUT (6-850 MCM 69 kV LPOF cables in duct bank).

6.4 Correlation Between Computer Output and Field Measurement.

Some conductor current and cable surface temperature measurements were taken on a section of ductline with a cable configuration similar to that discussed in section 6.3. The test location was 30 feet south of manhole X4, King Street south of William, on the Winnipeg Hydro 69 kV subtransmission system. Since these circuits are networked with other circuits on the subtransmission system, and in view of the dynamic nature of the load currents on the power system, a constant load cycle on the cables could not be maintained. Note that the analytical procedures discussed in this thesis are based on steady state conditions, and this condition is never really achieved in an actual cable installation unless the cable system is isolated and the load currents are controlled. Therefore, the information presented here only represents typical results for a working cable system.

The cable load characteristics used in the computation are for the 24 hour period preceding the cable surface temperatures being measured. Actual earth ambient temperatures were not recorded. However, measurements taken in previous years provided typical temperatures to be expected during the tests. Again, because of lack of equipment, no earth thermal resistance measurements were taken. Since cable ratings on the Winnipeg Hydro system are based on an earth thermal resistance of 90 ^{o}C cm/W,

this value is used in cases 1 and 2 to test the correlation between the measured cable surface temperature, T_s, and calculated temperatures. The averaged result of the measurements and computer calculations are shown in Table 6.2.

Case	Circuit	Ambient Temp, ^{o}C	Measured			Calculated	
			I,A	Fld,p.u.	T_s, ^{o}C	T_c, ^{o}C	T_s, ^{o}C
1 *	W5	0.0	120	0.61	5.0	5.0	4.0
	W6	0.0	290	0.81	6.0	9.0	5.0
2 *	W5	+7.0	390	0.66	18.5	21.0	14.0
	W6	+7.0	240	0.66	18.5	17.0	13.0
3 **	W5	+7.0	390	0.66	18.5	28.0	19.0
	W6	+7.0	240	0.66	18.5	23.0	18.0

$*\bar{\rho}_e = 90\ ^{o}C\ cm/W$, $**\ \bar{\rho}_e = 180\ ^{o}C\ cm/W$

TABLE 6.2 CORRELATION BETWEEN FIELD MEASUREMENT AND COMPUTATION

Reasonable correlation is achieved in case 1 when the load currents are small. However, in case 2, taken approximately two months later, and with higher load currents, the difference between measured and calculated cable surface temperatures is greater. If it is assumed that $\bar{\rho}_e$ is higher, 180 ^{o}C cm/W as shown in case 3, closer correlation is achieved. However, other parameters such as varying load characteristics, earth ambient temperature variations, and assumptions made when developing the

theoretical calculation affect the final results.

From this illustration, one concludes that detailed testing should be conducted on a duct bank where cable load characteristics, earth ambient temperature, and the overall thermal environment may be controlled and monitored. Results may be analyzed to varify the accuracy and gain confidence in the computation method presented in this thesis.

One also concludes that conservative estimates should be made when determining power cable ampacities theoretically. For example, in case 2, the measured cable temperatures were higher than the calculated values. By interpolating from Table 6.1, the theoretical rating for these cables is approximately 750 amps based on IPCEA and $\bar{\rho}_e = 90$. If the cables were loaded to 750 amps, one might expect that they would exceed their allowable temperature limits based on the measurement trend in case 2. Therefore, caution must be exercised when rating cables to ensure that they are not rated above their thermal limits.

CHAPTER 7

CONCLUSIONS AND RECOMMENDATIONS

Listed here are the important conclusions of the thesis, and recommendations for continuing further development of the project.

7.1 Conclusions

1. The analytical technique developed in this thesis is effective in analyzing a variety of cable system conditions under steady state conditions. Some typical situations include the following:

   i. New installations-by specifying cable operating temperatures, the cable ampacities may be calculated.

   ii. Existing installations - by knowing the cable load characteristics from field measurement, cable operating temperatures may be calculated and compared with allowable temperature limits specified by cable manufactures.

   iii. Existing installations - by knowing the load characteristics for all other circuits, the ampacity of a particular circuit may be calculated based on its allowable temperature limit. This portion of the calculation is useful when determining steady state emergency ratings for particular circuits in a large duct bank.

2. The number of cables contained in a duct bank, the conductor size, and cable position significantly affect

the allowable ampacity of cables. The physical configuration of the duct bank, duct spacing beyond approximately twelve inches and duct depths beyond approximately six feet have a lesser effect on cable ampacities. When designing a new cable installation every effort should be made to maximize the cable ampacity by selecting the best combination of parameters.

3. The analytical procedure presented here is equally accurate with any combination of conductor temperatures or currents being specified for the cable system.

4. The computer program developed in this thesis is a versatile tool for analyzing the ampacity and thermal performance of real cable systems. However, it is not intended to provide specific ratings for cables unless the user has a thorough knowledge the thermal and operating characteristics of the cable system being investigated. This procedure does not account for mechanical limitations of the cable caused by thermal expansion, or the ratings of potheads, joints, or different cable environments. Only after each of these has been investigated can a cable be rated with confidence.

5. Conservative assumptions regarding the cable operating constraints should be made when little is known about the cable system.

7.2 Recommendations

1. The analysis should be extended to include transient response, the effect of cold load pick up, and the effects of forced cooling in multi-duct systems.
2. Optimizing techniques should be applied to the analysis so that new and existing installations could be designed and operated to maximize equipment performance.
3. The analysis should be extended to include other types of cables and installations.
4. Extensive tests should be conducted on a duct bank installation to verify the results of the analysis presented. Preferably, a ductline should be constructed where the thermal and operating characteristics of the facility could be controlled and monitored.

This thesis has attempted to acquaint the reader with a procedure which may be used to investigate the performance of power cables in underground systems. The emphasis has been on presenting the theoretical background for many of the equations, and then developing a versatile tool for analyzing actual systems. It is hoped that the reader has found the information compiled in this thesis understandable and informative.

REFERENCES

(1) Edison Electric Institute Transmission and Distribution Committee, "Underground Systems Reference Book", Edison Electric Institute, 1957, Chapter 2.

(2) Hayt, Jr. William H., "Engineering Electromagnetics", McGraw-Hill Book Company, 1967, pp. 342-348.

(3) Insulated Power Cable Engineers Association (IPCEA), "Power Cable Ampacities, Volume I - Copper Conductors", AIEE Pub. No. S-135-1, IPCEA Pub. No. P-46-426, 1962.

(4) Dwight, H. B., "Skin Effect and Proximity Effect in Tubular Conductors", AIEE Transactions, Vol. 41, 1922, pp. 189-198.

(5) Arnold, A.M.H., "Eddy Current Losses in Multi-core paper Insulated Lead Covered Cables, Armoured and Unarmoured, Carrying Balanced Three Phase Current" Journal, Institute of Electrical Engineering, London, England, part I, Feb. 1941, pp. 52-63.

(6) Simmons, D.M., "Cable Geometry and the Calculation of Current Carrying Capacity", AIEE Transactions, Volume, 1923, pp. 600-620.

(7) Canada Wire and Cable Company Limited, "Power Cable Handbook No. P.C. 40", pp. 236.

(8) Simmons, D.M., "Calculation of Electrical Problems of Underground Cables", The Electric Journal, May to November, 1932.

(9) Neher, J. H. and McGrath, M.H., "The Calculation of the Temperature Rise and Load Capability of Cable Systems", AIEE Transactions, Vol.76, 1957, pp. 752-772.

(10) Neher, J.H., "The Temperature Rise of Buried Cables and Pipes", AIEE Transactions, Volume 68, 1949, pp. 9-21.

(11) Neher, J.H., "The Temperature Rise of Cables in a Duct Bank", Ibid, pp. 540-549.

(12) "The Effect of Loss Factor on the Temperature Rise of Pipe Cables and Buried Cables", AIEE Committee Report, AIEE Transactions, Volume 72, pt. III, 1953, pp. 530-535.

(13) Shanklin, G.B., and Buller, F.H.,. "Cyclical Loading of Buried Cable and Pipe Cable", Ibid, pp. 536-540.

(14) Neher, J.H., "Procedures for Calculating the Temperature Rise of Pipe Cable and Buried Cables for Sinusoidal and Rectangular Loss Cycles", Ibid, pp. 541-544.

(15) Wiseman, R. J., "An Empiracle Method For Determining Transient Temperatures of Buried Cable Systems", Ibid, pp. 545-562.

(16) Manning, L. W., "Load Characteristics", Distribution Systems, Westinghouse Electric Corporation, 1965.

(17) "Calculation of the Continuous Current Rating of Cables (100% Load Factor)", International Electrothechnical Commission, Publication 287, 1969, (Revised Feb. 1980, Reference No. 20A78).

(18) Keyhani, A. and Weeks, W.L., "Ampacities of Underground Cable Systems", paper no. 39-73, Perdue University, School of Electrical Engineering, West Lafayette, Indiana, 1973.

(19) Kreyszig, Erwin, "Advanced Engineering Mathematics", John Wiley and Sons, Inc., New York, 1967, pp. 398-400.

(20) Bukoski, D. F., "The Ampacity and Thermal Performance of Distribution Cable in Underground Systems - User Manual, Computer Program SLVCBL", Technical Report No. PGP 81-01 , Department of Electrical Engineering, University of Manitoba.

(21) Ford, G.L., Steinmanis, J.E., "Climate is Important In Thermal Design of Underground Transmission Systems", Ontario Hydro Research Division, Transmission and Distribution, March, 1980, pp. 48-52.

(22) Leach, John B., "Ampacity Determination of Underground Cable Systems in Power Distribution Substations", Technical Paper, Public Service Company of Oklahoma, 1979.

(23) Mason, V.V., and Kurtz, M., " Rapid Measurement of the Thermal Resistivity of Soil", AIEE Transactions, Vol. 71 , 1952, pp. 570-576.

(24) Buggs, S.A., Chu, F.Y. and Griffin, J.D., "Instrument Measures Soil Thermal Properties", Transmission and Distribution, February, 1980, pp. 24-30.

(25) Staple, John, "Soil Thermal Resistivity Measured Simply and Accurately", AIEE Transactions, Volume 89, 1970, pp. 297-304.

(26) Buller, F.H. and Neher, J.H., "The Thermal Resistance Between Cables and a Surrounding Pipe or Duct Wall", AIEE Transaction, Volume 69, Pt. I, 1950, pp. 342-349.

(27) Greebler, P. and Barnett, G.F, "Heat Transfer Study on power Cable Ducts", AIEE Transactions, Volume 69, Pt. I, 1950, pp. 357-367.

SELECTED BIBLIOGRAPHY

(1) Kellow, M., "The Forced Cooling of Distribution Cables in a Duct Bank; Analysis of Cable Ampacity and Thermal Performance", CEA Research Report #77-38, April, 1980.

(2) Gryzbowski, S. and Poltz, J., "Continuous Current Rating of Single Core Cables in Trefoil Formation", Technical University of Poznan, Poland.

(3) Weeks, W. L. and Wiley, R. G., "Ampacities of Underground Cables in Real Systems", paper, Edison Electrical Institute, May, 1974.

(4) Alex, P. A., "New Cable - Loading Concept Explored", Electrical World, January, 1976, pp. 36-39.

(5) Gronin, J. C. and Conangla, A., "Heat-Flux Temperature Relationships For Closely Spaced Underground Power Transmission Conductors", IEEE paper 70, TP 551-PWR.

(6) Jackson, R. J., "Eddy Current Losses in Unbouded Tubes", IEE Proceedings, Volume 122, No. 5, 1975, pp. 551-557.

(7) Goldenberg, H., "The Calculation of Continuous Current Ratings and Rating Factors for Transmission and Distribution Cables", The British Electrical and Allied Industries Research Association, Technical Report F/T187, 1958.

(8) Jacob, M., "Elements of Heat Transfer", John Wiley and Sons Inc., 3rd Edition, 1961.

(9) Fink, L. H. and Smerke, J. J., "Control of the Thermal Environment of Buried Cable Systems", AIEE Transaction, Volume 77, Part III, 1958, pp 161-168.

(10) Barnes, C. C., "Power Cables", Chapman and Hall Ltd., London 2nd Edition, 1966.

(11) Bailey, N. P., "Heat Flow From Underground Electric Power Cables", AIEE Transaction, Volume 48, January, 1929, pp. 156-165.

(12) "Soil Thermal Characteristics in Relation to Underground Power Cable", AIEE Committee Report, Ibid., Volume 79, Part III, 1960, PP. 792-856.

APPENDIX A1

Sheath Circulating Current

$$I_s = \frac{V_m}{Z_s} \quad A \qquad \text{A1.1}$$

where I_s is the sheath current,

V_m is the induced sheath voltage due to coupling between the sheath and phase conductor, and Z_s is the sheath impedance. Z_s may be expressed as

$$Z_s = \sqrt{X_m 2 + R_s 2} \ \Omega/ft \qquad \text{A1.2}$$

where X_m = sheath mutual reactance

R_s = sheath dc resistance

also $$V_m = I_c X_m \ \text{volts} \qquad \text{A1.3}$$

where I_c = conductor current

Combining equations A1.1, A1.2 and A1.3,

$$I_s = I_c \frac{X_m}{X_m 2 + R_s 2} \ A \qquad \text{A1.4}$$

APPENDIX A2

The Heat Transfer Equation

Referring to figure 3.2(b) and applying equation 3.1, the rate of heat energy which flows radially through the differential volume $2\pi r \cdot \Delta r \cdot l$ is

$$q = -k \quad 2\pi r \; l \quad \frac{\Delta T}{\Delta r} \quad W \qquad \text{A2.1}$$

The negative sign indicates that the temperature decreases as the distance from the reference point in the direction of heat flow increases. r represents the variable radius of the insulation and l the length of the section. For simplification, a unit length of cable is to be selected so that l is unity.

Equation A2.1 may be expressed as

$$\frac{q}{l} = -k \quad 2\pi r \quad \frac{dt}{dr} \quad W/ft \qquad \text{A2.2}$$

Defining $Q = \frac{q}{l} \quad \frac{Btu}{hr.\text{-}ft.}$ and rewriting A2.2,

$$Q = -k \; 2\pi r \quad \frac{dt}{dr} \quad W/ft$$

Expressed in differential form, and defining thermal resistivity $\bar{\rho} = \frac{1}{k}$

$$\frac{dt}{dr} + \frac{Q\bar{\rho}}{2\pi r} = 0 \qquad \text{A2.3}$$

Solving for dt and integrating,

$$t = -\frac{Q\bar{\rho}}{2\pi} \ln(r) + C \qquad \text{A2.4}$$

When $r = r_1$, $t = t_1$ and when $r = r_2$, $t = t_2$.

Substituting into equation A2.4

$$t_1 = - \frac{Q\bar{\rho}}{2\pi} \ln (r_1) + C$$

$$t_2 = - \frac{Q\bar{\rho}}{2\pi} \ln (r_2) + C$$

Eliminating C,

$$\Delta T = t_1 - t_2 = \frac{Q\bar{\rho}}{2\pi} \ln \left[\frac{r_2}{r_1}\right] \quad ^{o}C$$

Defining $\bar{R} = \frac{\bar{\rho}}{2\pi} \ln \left[\frac{r_2}{r_1}\right] \quad ^{o}C \text{ ft/W}$ A2.5

$$\Delta T = Q \cdot \bar{R} \quad ^{o}C$$

$\bar{\rho}$ is usually expressed as cm/watt/^{o}C in the literature; Converting equation A2.5 to British units, of measurement and expressing cables heat loss as W watts/conductor foot,

$$\bar{R} = \frac{\bar{\rho}}{2\pi} \ln \left[\frac{r_2}{r_1}\right] \cdot \frac{1}{30.48 \frac{cm}{ft}} \quad ^{o}C \text{ cm/W}$$

$$= .00522\, \bar{\rho} \ln \left[\frac{r_2}{r_1}\right] \quad ^{o}C \text{ ft/W}$$

$\ln (r_2/r_1)$ involves the cable insulation shape and is called the Geometric Factor G. Therefore

$$\bar{R} = .00522\, \bar{\rho}\, G \quad ^{o}C \text{ ft/W} \qquad \text{A2.7}$$

and

$$\Delta T = W \cdot \bar{R} \quad ^{o}C \qquad \text{A2.8}$$

APPENDIX A3

Equivalent Isothermal Radius for a Rectangular Duct Bank(9)

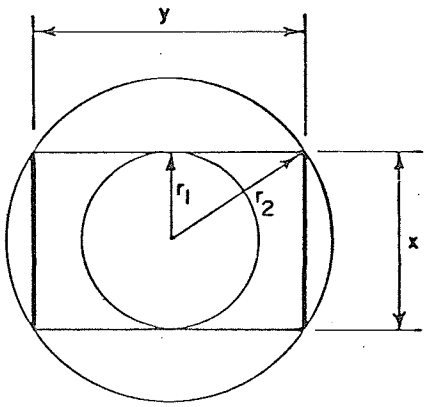

FIGURE A3.1 - RECTANGULAR DUCT BANK

GIVEN: rectangular duct bank
X = smaller dimension, in
Y = larger dimension, in

$$A_1 = \pi r_1^2$$

$$A_2 = \pi r_2^2$$

$$A_3 = XY$$

r_1 = radius of circle inscribed within duct bank

$= X/2$

r_2 = radius of circle embracing four corners of duct bank

$$= \frac{\sqrt{X^2 + Y^2}}{2}$$

Assume: a circle of radius r_b lies between r_1 and r_2 and

the magnitude of r_b divides the thermal resistance between r_1 and r_2 in direct relation to the occupied and unoccupied portions of the heat field between r_1 and r_2.

From equation 3.3

$$\Delta T_1 = \frac{Q \bar{\rho}_c}{2\pi} \ln \left[\frac{r_2}{r_1}\right], \text{ and } \Delta T_2 = \frac{Q \bar{\rho}_c}{2\pi} \ln \left[\frac{r_b}{r_1}\right]$$

$$\frac{\Delta T_2}{\Delta T_1} = \frac{\ln \left[r_b/r_1\right]}{\ln \left[r_2/r_1\right]}$$

$$= \frac{A_3 - A_1}{A_2 - A_1} = \frac{XY - \pi r_1^2}{\pi r_2^2 - \pi r_1^2} \qquad \text{A3.1}$$

$$\ln \left[\frac{r_b}{r_1}\right] = \frac{XY - \pi r_1^2}{\pi (r_2^2 - r_1^2)} \ln \left[\frac{r_2}{r_1}\right]$$

Solving for r_b,

$$\ln (r_b) = \frac{XY - \pi r_1^2}{\pi (r_2^2 - r_1 2)} \ln \left[\frac{r_2}{r_1}\right] + \ln (r_1) \qquad \text{A3.2}$$

Substituting $r_1 = \frac{X}{2}$, $r_2 = \frac{\sqrt{X^2 + Y^2}}{2}$;

$$r_b = \ln^{-1} \left[\frac{1}{2} \cdot \frac{X}{Y} \cdot \left[\frac{4}{\pi} - \frac{X}{Y}\right] \ln \left[1 + \frac{Y^2}{X^2}\right] + \ln \left[\frac{X}{2}\right]\right] \qquad \text{A3.3}$$

or

$$D_b = 2 r_b \text{ in} \qquad \text{A3.4}$$

APPENDIX A4

Thermal Resistance Between A Cylindrical Radiator and Ambient Earth(10)

Assume a long straight filament continuously radiating Q watts per unit length located in an infinite medium of constant thermal resistance at point O in figure A4.1. The differential equation describing the heat flow as a function of temperature T at a distance r from O is defined by equation A2.3 as

$$\frac{dt}{dr} + \frac{Q\bar{\rho}}{2\pi r} = 0 \qquad \text{A2.3}$$

A temperature rise at a point P, a distance d from O is found by integrating equation A2.3 between the limits $r_1 = \infty$ and $r_2 = d$, i.e.

$$\Delta T = \int_{r_1=\infty}^{r_2=d} -\frac{Q\bar{\rho}}{2\pi}\,\frac{dr}{r} \qquad \text{A4.1}$$

By applying the method of Images, assume a similar parallel filament located at O' continuously absorbing -Q watts per unit length,

$$\Delta T' = \int_{r_1=\infty}^{r_2=d'} \frac{Q\bar{\rho}}{2\pi}\,\frac{dr}{r} \qquad \text{A4.2}$$

If the two heat flows operate simultaneously, by the Superposition theorem,

$$\Delta T_p = \Delta T + \Delta T'$$

$$= \frac{Q\bar{\rho}}{2\pi} \ln\left[\frac{d'}{d}\right] \qquad \text{A4.3}$$

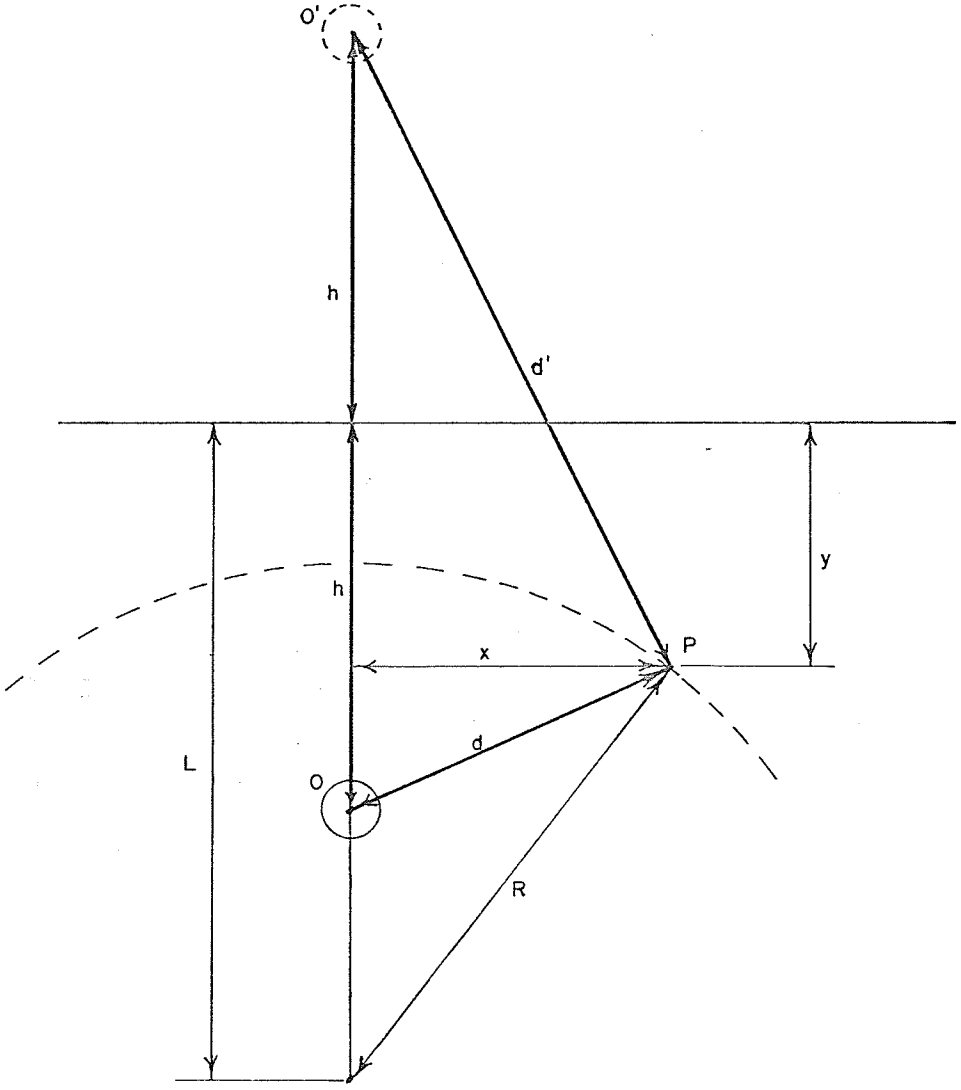

FIGURE A4.1 - GEOMETRY OF A CYLINDRICAL THERMAL RADIATOR.

letting $\frac{d'}{d} = k$ and applying the rectangular co-ordinates in figure A4.1,

$$d'^2 = (h + Y)^2 + X^2; \quad d^2 = (h - Y)^2 + X^2$$

$$\frac{d'^2}{d^2} = k^2 = \frac{(h + Y)^2 + X^2}{(h - Y)^2 + X^2} \qquad \text{A4.4}$$

From which,

$$X^2 + \left[Y - h \cdot \frac{k^2 + 1}{k^2 - 1}\right]^2 + X^2 = 4h^2\left[\frac{k}{k^2 - 1}\right]^2 \qquad \text{A4.5}$$

This is the equation of a circle with radius

$$R = 2h \cdot \frac{k}{k^2 - 1} \qquad \text{A4.6}$$

whose centre lies at a distance below the origin

$$L = h \cdot \frac{k^2 + 1}{k^2 - 1} \qquad \text{A4.7}$$

From equations A4.6 and A4.7,

$$L^2 - R^2 = h^2 \qquad \text{A4.8}$$

For various constant values of ΔT_p the locus of point p is a family of eccentric cylinders (circles in section of figure A4.1) about point O, if ΔTp is positive, and about O' if ΔTp is negative. The isothermal cylinders increase in diameter as the value of d'/d decreases. When d'/d = 1 the isothermal cylinders merge into a plain bisecting and perpendicular to the line 0 - 0'. $\Delta Tp = 0$ for all points of p on this isothermal plain, which can be equated to the earth's surface.

Solving equations A4.6 and A4.7 for K in terms of L/R,

$$k^2 - \frac{2KL}{R} + 1 = 0 \qquad \text{A4.9}$$

Using the binomial theorem to solve for K,

$$k = \frac{d'}{d} = \frac{L \pm \sqrt{L^2 - R^2}}{R}$$

Substituting into equation A4.3,

$$\Delta T = \frac{Q\bar{\rho}}{2\pi} \ln \left[\frac{L + \sqrt{L^2 - R^2}}{R} \right] {}^{o}C \qquad \text{A4.10}$$

This equation, known as the long form of the Kennelly formula, gives the temperature rise at the surface of a cylindrical radiator of radius R. Expressing equation A4.10 in terms of the earth thermal resistance $\bar{R}_e$, the equivalent duct bank radius r_b and the depth to its centre L_b, and converting $\bar{\rho}$ ^{o}C cm/watt to British units of measure,

$$\Delta T = Q \bar{R}_e \ {}^{o}C \qquad \text{A4.11}$$

where

$$\bar{R}_e = .00522 \ \bar{\rho}_e \ \ln \left[\frac{L_b + \sqrt{L^2_b - r_b{}^2}}{r_b} \right] {}^{o}C \text{ ft/W} \qquad \text{A4.12}$$